Study of $B_c^+ \to J/\psi D_s^{(*)+}$ decays

Y. Fang

IHEP

July 15, 2019

Outline

Motivation

- B_c^+ meson is a heavy meson consisting of two heavy quarks with different flavors
- Both b and c quarks may be involved in their weak decays

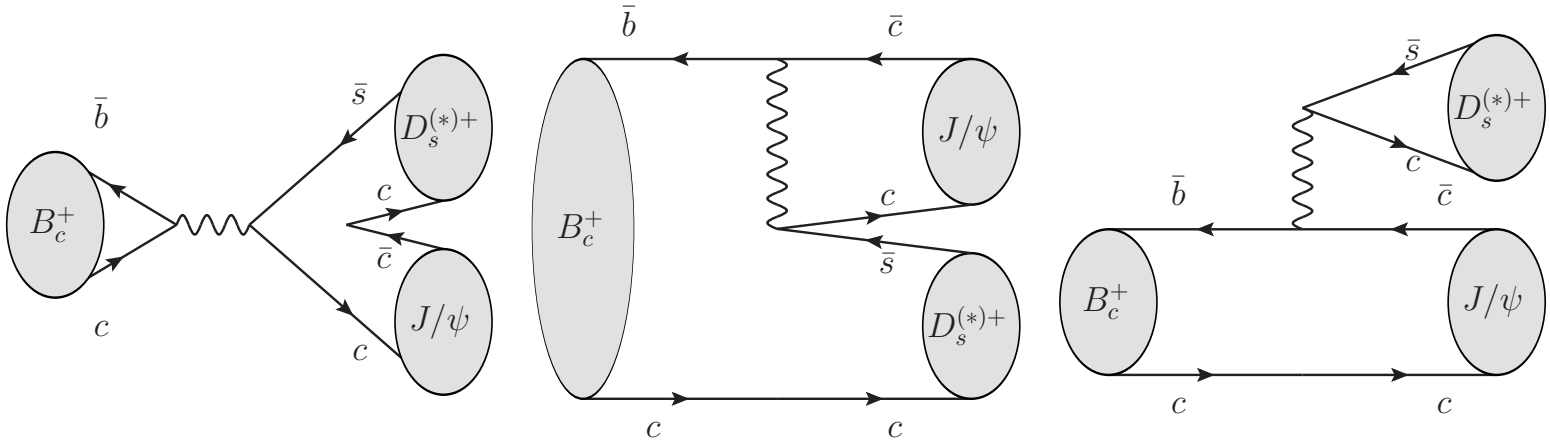

- Test various QCD approaches

Previous studies

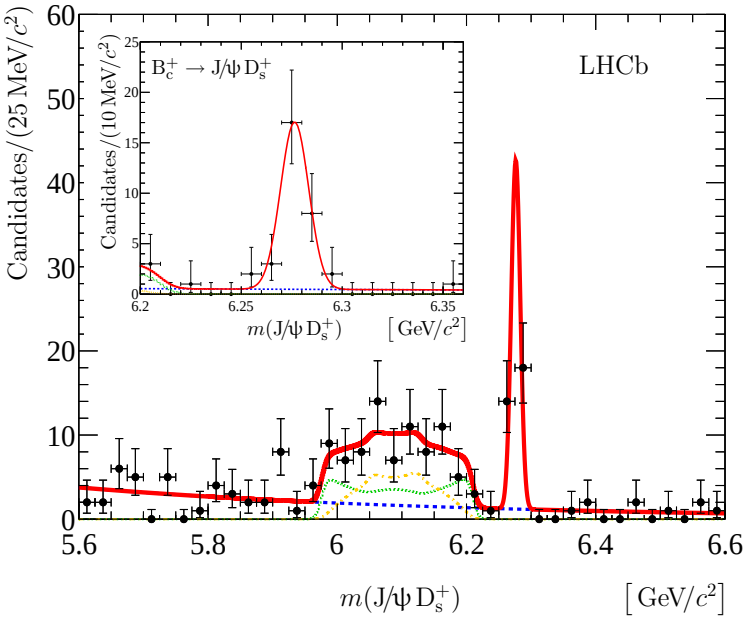

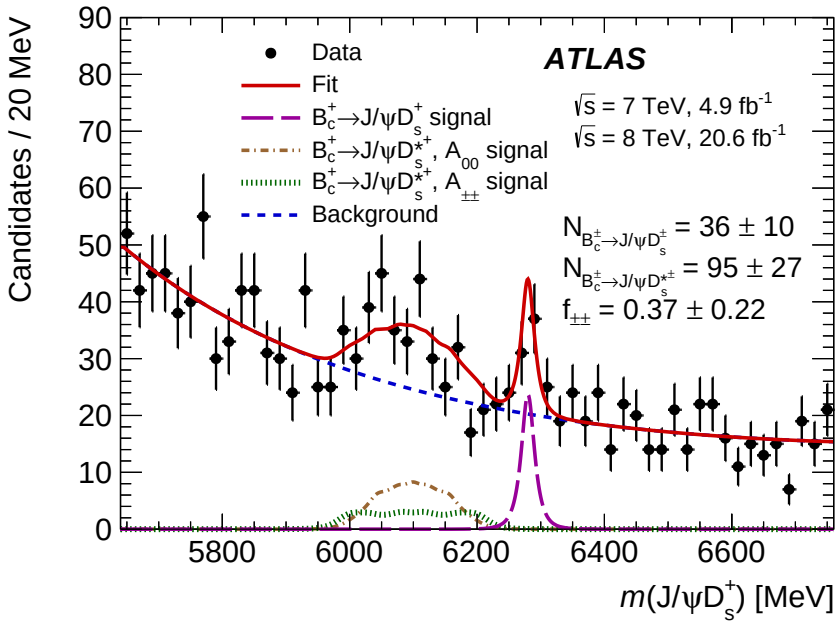

Experiment	LHCb [PRD **87**, 112012 (2003)]	ATLAS [EPJC **76**, 4 (2016)]
Luminosity	3 fb^{-1} at 7, 8 TeV	25.5 fb^{-1} at 7, 8 TeV
$m_{B_c^+}$ [MeV]	6276.28 ± 1.44	6279.9 ± 3.5
$\sigma_{B_c^+}$ [MeV]	7.0 ± 1.4	7.9 ± 3.0
$N_{B_c^+ \to J/\psi D_s^+}$	28.9 ± 5.6	36 ± 10
$N_{B_c^+ \to J/\psi \pi^+}$	3009 ± 79	1140 ± 120
Systematic uncertainty	8.4%	10.1%
$\frac{B_c^+ \to J/\psi D_s^+}{B_c^+ \to J/\psi \pi^+}$	$2.90 \pm 0.57 \pm 0.24$	$3.8 \pm 1.1 \pm 0.4 \pm 0.2$

Data set

- **Software version: Athena release 21.2**
- **Derivation:** `BPHY15`
  - **data15_13TeV.period*.physics_Main.PhysCont.DAOD_BPHY15.grp15_v01_p3730**
  - **data16_13TeV.period*.physics_Main.PhysCont.DAOD_BPHY15.grp16_v01_p3730**
    data16_13TeV.period*.physics_BphysDelayed.PhysCont.DAOD_BPHY15.grp16_v01_p3730
  - **data17_13TeV.period*.physics_BphysLS.PhysCont.DAOD_BPHY15.grp17_v01_p3730**
  - **data18_13TeV.period*.physics_BphysLS.PhysCont.DAOD_BPHY15.grp18_v01_p3760**
- **Good Run List with the detector in the "All Good" status:**
  - **data15_13TeV.periodAllYear_DetStatus-v89-pro21-02_Unknown_PHYS_StandardGRL_All_Good_25ns.xml**
  - **data16_13TeV.periodAllYear_DetStatus-v89-pro21-01_DQDefects-00-02-04_PHYS_StandardGRL_All_Good_25ns.xml**
  - **data17_13TeV.periodAllYear_DetStatus-v99-pro22-01_Unknown_PHYS_StandardGRL_All_Good_25ns_Triggerno17e33prim.xml**
  - **data18_13TeV.periodAllYear_DetStatus-v102-pro22-04_Unknown_PHYS_StandardGRL_All_Good_25ns_Triggerno17e33prim.xml**

After applying the GRL, the integrated luminosity of the 2015+2016 dataset is 36.2 **fb**$^{-1}$**,** 44.3 **fb**$^{-1}$ **for the 2017 dataset and** 58.5 **fb**$^{-1}$ **for 2018 dataset, giving a total integrated luminosity of** 139.0 ± 2.4 **fb**$^{-1}$**.**

MC simulation

- **The MC samples are generated with Pythia 8.212. The generator BCVEGPY is used to simulate the production of B_c^+ mesons. The decays of heavy-flavoured hadrons are simulated with EvtGen.**
- **The generated events were passed through a full simulation of the detector using the ATLAS simulation framework based on Geant 4 and processed with the same reconstruction algorithms as were used for the data.**

Decay	DSID	Campaign	p-tag
$B_c^+ \to J/\psi D_s^+$	300608	mc16a	e7347_a875_r9364_p3795
	300609	mc16a	e7347_a875_r9364_p3795
$B_c^+ \to J/\psi D_s^{*+}$, $\mathcal{A}_{00}$	300610	mc16a	e7347_a875_r9364_p3795
	300611	mc16a	e7347_a875_r9364_p3795
$B_c^+ \to J/\psi D_s^{*+}$, $\mathcal{A}_{++}$	300612	mc16a	e7347_a875_r9364_p3795
	300613	mc16a	e7347_a875_r9364_p3795
$B_c^+ \to J/\psi D_s^{*+}$, $\mathcal{A}_{--}$	300614	mc16a	e7347_a875_r9364_p3795
	300615	mc16a	e7347_a875_r9364_p3795
$B_c^+ \to J/\psi \pi^+$	300600	mc16a	e7012_a875_r9364_p3851
		mc16d	e7012_a875_r10201_p3851
		mc16e	e7012_a875_r10724_p3851
	300601	mc16a	e7012_a875_r9364_p3851
		mc16d	e7012_a875_r10201_p3851
		mc16e	e7012_a875_r10724_p3851
$B_c^{*+} \to B_c^+\gamma$, $B_c^+ \to J/\psi \pi^+$	300602	mc16a	e7012_a875_r9364_p3851
		mc16d	e7012_a875_r10201_p3851
		mc16e	e7012_a875_r10724_p3851
	300603	mc16a	e7012_a875_r9364_p3851
		mc16d	e7012_a875_r10201_p3851
		mc16e	e7012_a875_r10724_p3851

Triggers

Trigger	Fraction
2015 data, physics_Main, run 266904–284484	
HLT_mu6_mu4_bJpsimumu_noL2	0.999928
HLT_2mu4_bJpsimumu_noL2	0.799727
2016 data, physics_Main, run 296939–302925	
HLT_mu6_mu4_bJpsimumu	0.363558
HLT_mu10_mu6_bJpsimumu	0.999368
HLT_2mu6_bJpsimumu	0.654487
HLT_mu20_2mu0noL1_JpsimumuFS	0.894017
HLT_mu6_2mu4_bJpsi	0.64169
2016 data, physics_Main, physics_BphysDelayed, run 302956–311481	
HLT_mu20_2mu0noL1_JpsimumuFS	0.799626
HLT_mu6_mu4_bBmumux_BsmumuPhi_delayed	0.349642
HLT_mu20_nomucomb_mu6noL1_nscan03	1
HLT_2mu6_bJpsimumu_delayed	0.988621
HLT_mu6_mu4_bJpsimumu_Lxy0_delayed	0.359082
HLT_mu6_nomucomb_2mu4_nomucomb_delayed_L1MU6_3MU4	0.90415
HLT_2mu4_bBmumux_BsmumuPhi_delayed_L1BPH-2M8-2MU4	0.142957
2017 data, physics_BphysLS, run 325713–341649	
HLT_2mu6_bJpsimumu_L1BPH-2M9-2MU6_BPH-2DR15-2MU6	0.970976
HLT_mu6_mu4_bBmumux_BsmumuPhi_L1BPH-2M9-MU6MU4_BPH-0DR15-MU6MU4	0.788403
HLT_mu11_mu6_bDimu	0.999887
HLT_3mu4_bDimu	1
2018 data, physics_BphysLS, run 348197–364292	
HLT_2mu6_bJpsimumu_L1BPH-2M9-2MU6_BPH-2DR15-2MU6	1
HLT_mu6_mu4_bBmumux_BsmumuPhi_L1BPH-2M9-MU6MU4_BPH-0DR15-MU6MU4	0.853167
HLT_mu11_mu6_bDimu	1
HLT_2mu4_bJpsimumu_Lxy0_L1BPH-2M9-2MU4_BPH-0DR15-2MU4	0.0844957
HLT_3mu4_bJpsi	1
HLT_mu11_2mu4noL1_bNocut_L1MU11_2MU6	1

$B_c^+ \to J/\psi D_s^+$ selection criteria

- J/ψ **reconstruction**: vertex fit $\chi^2/N_{\rm dof} < 10$
  - Two combined muons
  - $2800 < m(\mu^+\mu^-) < 3400$ MeV
- D_s^+ **reconstruction**: tracks with opposite charges are assigned kaon mass hypotheses and combined in pairs to form ϕ candidates. An additional track is assigned a pion mass and combined with ϕ candidate to form a D_s^+ candidate.
  - Vertex fit $\chi^2/N_{\rm dof} < 5$
  - $|m(K^+K^-) - 1019.461| < 7$ MeV, $1930 < m(K^+K^-\pi^+) < 2010$ MeV
- B_c^+ **reconstruction**: perform cascade vertices fit with mass constraints on J/ψ and D_s^+ candidates
  - $\chi^2/N_{\rm dof} < 3$
  - $L_{xy}(B_c^+) > 0.10$ mm, $L_{xy}(D_s^+) > 0.15$ mm
  - $p_{\rm T}^{\rm refitted}(K/\pi) > 1$ GeV, $p_{\rm T}^{\rm refitted}(\mu) > 4$ GeV
  - $|\eta^{\rm refitted}(K/\pi)| < 2.5$, $|\eta^{\rm refitted}(\mu)| < 2.3$
  - $p_{\rm T}(B_c^+) > 15$ GeV, $|\eta(B_c^+)| < 2.0$
  - Transverse and longitudinal impact parameters: $|d_0^{\rm PV}(B_c^+)| < 0.1$ mm, $|z_0^{\rm PV}(B_c^+)\sin\theta(B_c^+)| < 0.5$ mm
  - $p_{\rm T}(B_c^+)/\sum p_{\rm T}({\rm trk}) > 0.10$, where the sum is taken over all tracks originating from PV
- **Veto** $B_s^0 \to J/\psi\phi$ **background**: candidates with $5340 < m(J/\psi\phi) < 5400$ MeV are rejected

$B_c^+ \to J/\psi D_s^+$ selection criteria

- $\cos\theta^*(\pi) < 0.8$, $\theta^*(\pi)$ is the angle between the pion momentum in the $K^+K^-\pi^+$ rest frame and the $K^+K^-\pi^+$ combined momentum in the lab frame
- $|\cos^3\theta'(K)| > 0.15$, $\theta'(K)$ is the angle between one of the kaons and the pion in the K^+K^- rest frame
- $\cos\theta^*(D_s^+) > -0.8$, $\theta^*(D_s^+)$ is the angle between the D_s^+ momentum in the rest frame of B_c^+, and the B_c^+ line of flight in the lab. frame
- $\cos\theta'(\pi) > -0.8$, $\theta'(\pi)$ is the angle between J/ψ momentum and the pion momentum in the $K^+K^-\pi^+$ rest frame

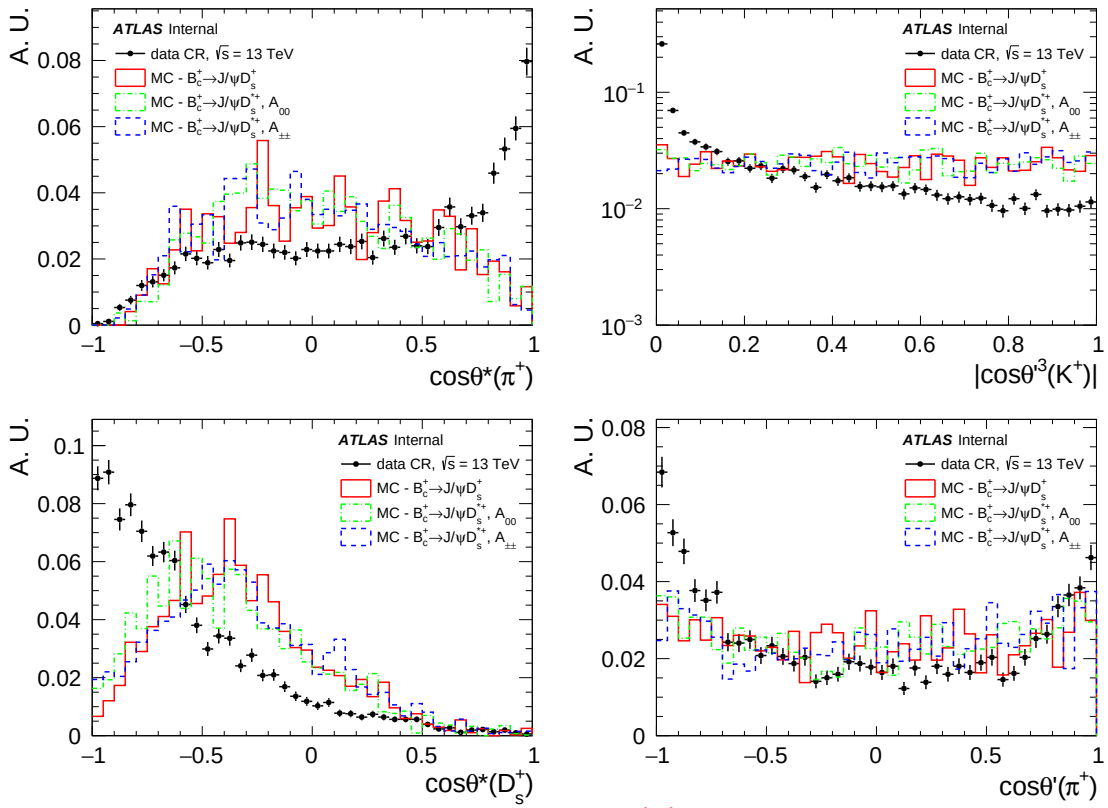

Invariant mass sepctrum

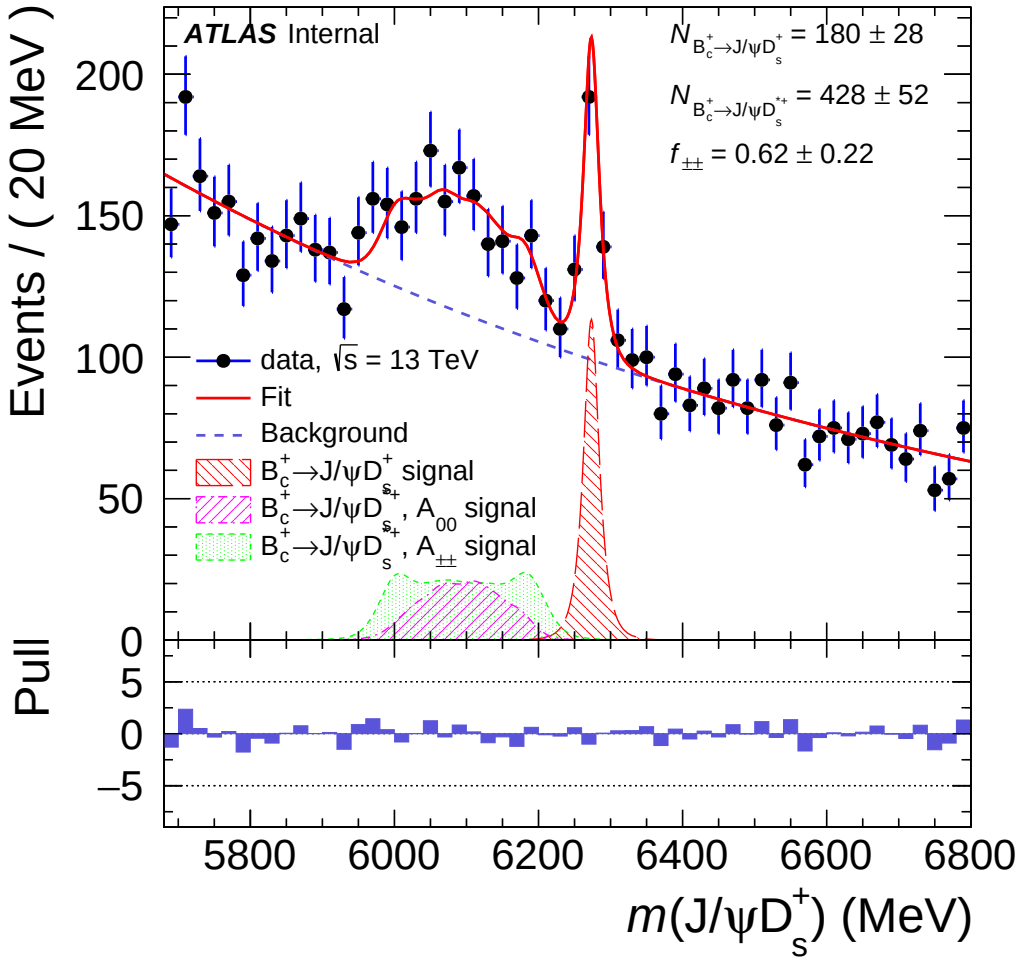

To extract the signal yields, an extended binned maximumlikelihood fit to the mass spectrum is performed.

Parameter	Value
$m_{B_c^+}$ [MeV]	6273.4 ± 1.9
$\sigma_{B_c^+}$ [MeV]	10.4 ± 2.1
$N_{B_c^+\to J/\psi D_s^+}$	180.3 ± 27.7
$N_{B_c^+\to J/\psi D_s^{*+}}$	427.7 ± 52.3
$f_{\pm\pm}$	0.62 ± 0.22

- $B_c^+ \to J/\psi D_s^+$ **signal PDF: modified Gaussian function**
- $B_c^+ \to J/\psi D_s^{*+}$ **signal PDF: kernel estimation from the MC simulated samples**
- **Combinatorial background PDF: exponential function**

$B_c^+ \to J/\psi\pi^+$ selection criteria

- B_c^+ **reconstruction**: perform vertex fit with mass constraint on J/ψ candidates
  - $\chi^2/N_{\rm dof} < 2$
  - $L_{xy}(B_c^+)/\sigma(L_{xy}(B_c^+)) > 3$, $0.2 < L_{xy}(B_c^+) < 10$ mm
  - $p_{\rm T}(B_c^+) > 15$ GeV, $p_{\rm T}^{\rm refitted}(\pi) > 3.5$ GeV, $p_{\rm T}^{\rm refitted}(\mu) > 4$ GeV
  - $|\eta(B_c^+)| < 2.0$, $|\eta^{\rm refitted}(\pi)| < 2.5$, $|\eta^{\rm refitted}(\mu)| < 2.3$
  - Transverse and longitudinal impact parameters: $|d_0^{\rm PV}(B_c^+)| < 0.1$ mm, $|z_0^{\rm PV}(B_c^+)\sin\theta(B_c^+)| < 0.5$ mm
  - $p_{\rm T}(B_c^+)/\sum p_{\rm T}({\rm trk}) > 0.15$, where the sum is taken over all tracks originating from PV
- **Angular cuts**:
  - $\cos\theta^*(\pi^+) > -0.8$, $\theta^*(\pi^+)$ is the angle between the π^+ momentum in the rest frame of B_c^+, and the B_c^+ line of flight in the lab. frame
  - $|\cos\theta'(\mu^+)| < 0.8$, where $\theta'(\mu^+)$ is the angle between muon momentum and the pion momentum in the J/ψ rest frame.

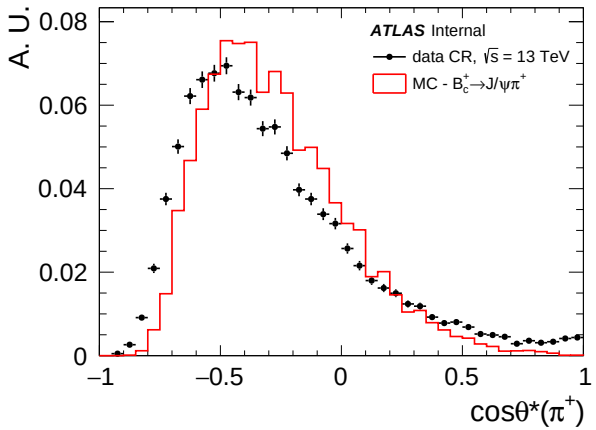

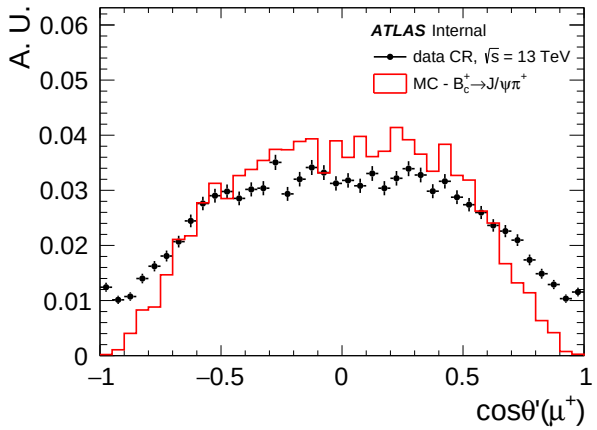

Invariant mass sepctrum

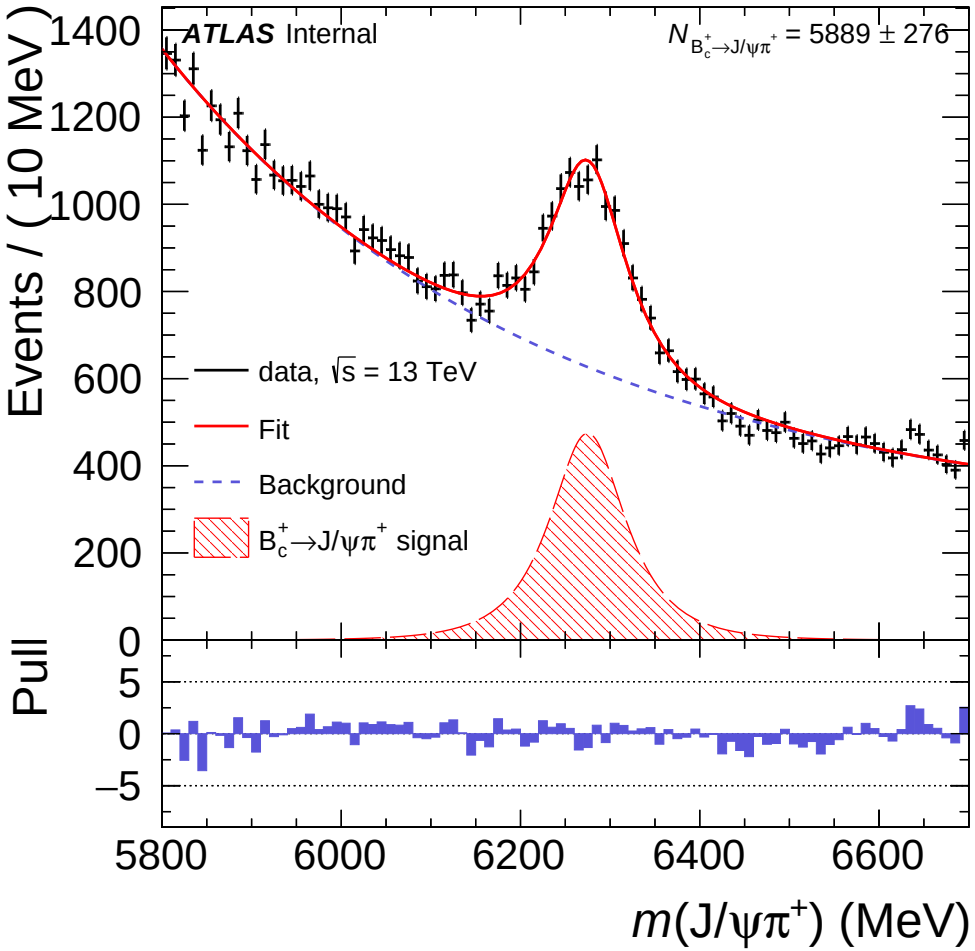

To extract the signal yields, an extended binned maximumlikelihood fit to the mass spectrum is performed.

Parameter	Value
$m_{B_c^+}$ [MeV]	6274.9 ± 1.6
$\sigma_{B_c^+}$ [MeV]	40.7 ± 1.9
$N_{B_c^+ \to J/\psi\pi^+}$	5889 ± 276

- $B_c^+ \to J/\psi\pi^+$ **signal PDF: modified Gaussian function**
- **Combinatorial background PDF: a two-parameter exponential function:** $\exp[a \cdot m(J/\psi\pi^+) + b \cdot m^2(J/\psi\pi^+)]$

Efficiencies

- **Due to the requirements on the muon kinematics applied in the MC at generator level, the acceptance of each decay mode $B_c^+ \to X$ (here X represents $J/\psi D_s^+$, $J/\psi \pi^+$, etc.) should be factorized as:**

$$\mathcal{A}_{B_c^+ \to X} = \mathcal{A}^{\mathbf{rec}}_{B_c^+ \to X} \times \mathcal{A}^{\mathbf{gen}}_{B_c^+ \to X}.$$

- **The factor $A^{\mathbf{rec}}_{B_c^+ \to X}$ represents a correction of the reconstructed and selected events number to the reconstruction range:**
  - $p_{\mathbf{T}}(B_c^+) > 15$ **GeV,** $|\eta(B_c^+)| < 2.0$,
  - $p_{\mathbf{T}}(\mu^\pm) > 4$ **GeV,** $|\eta(\mu^\pm)| < 2.3$,

  which is not acted by the generator level cuts
- **The acceptance $A^{\mathbf{gen}}_{B_c^+ \to X}$ is introduced to extrapolate beyond the muon kinematic cuts to the actual B_c^+ fiducial kinematic range**
  - $p_{\mathbf{T}}(B_c^+) > 15$ **GeV,** $|\eta(B_c^+)| < 2.0$,

  and is obtained from separate generator-level studies with high-statistics MC where no muon cuts are applied.

MC reweighting - Trigger reweighting

The weight for each simulated event is calculated based on lumiblock-by-lumiblock prescales taken from data with the following formula:

$$w = \frac{1}{\mathcal{L}} \sum_j \mathcal{L}_j \left(1 - \prod_i \left(1 - \frac{1}{P_j^i}\right)\right),$$

where P_j^i is the prescale factor of tigger i in the lumiblock j, $\mathcal{L}_j$ is the luminosity of the lumiblock j, and $\mathcal{L}$ is the total luminosity of the lumiblocks considered.

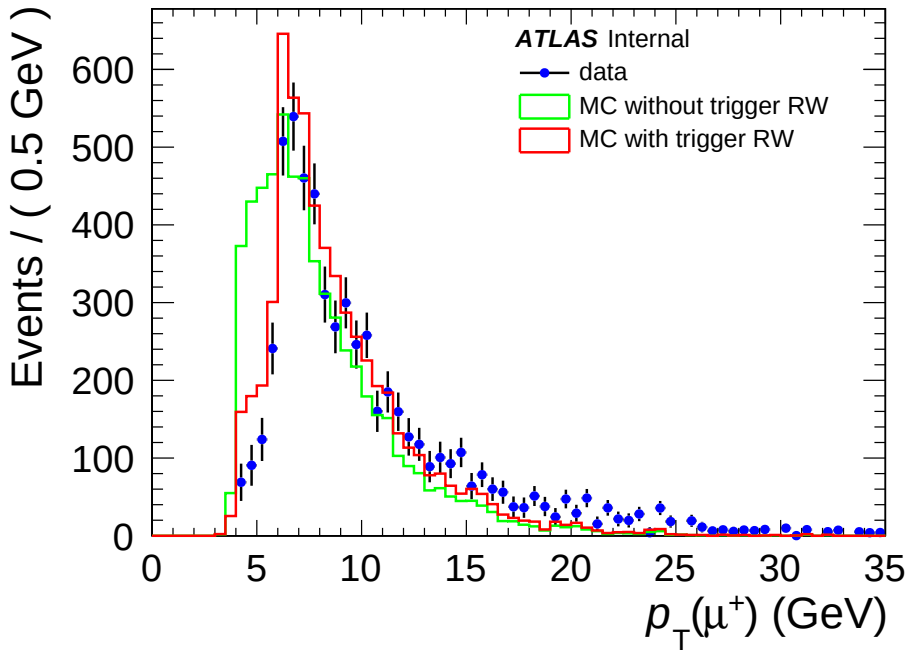

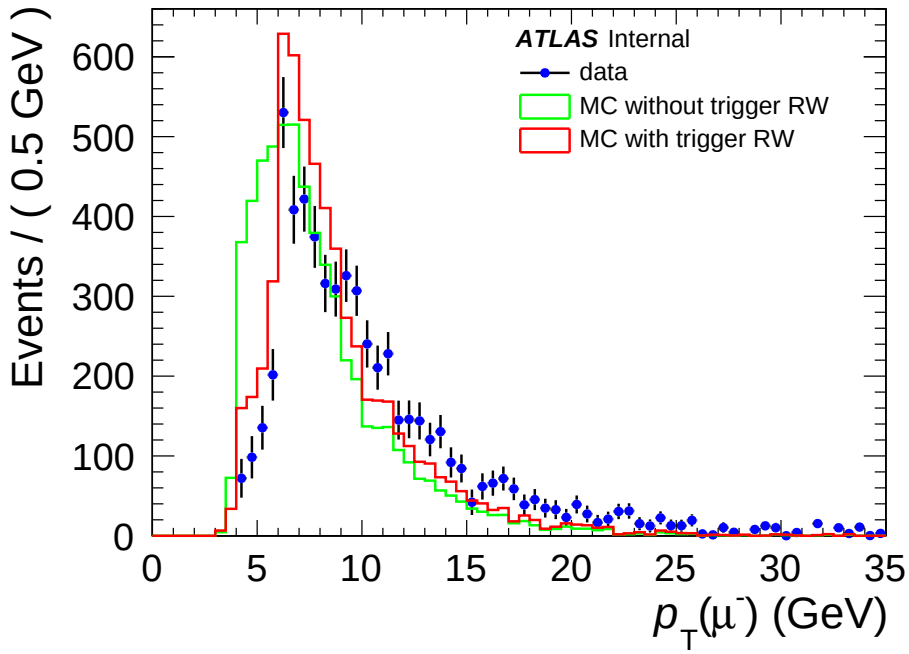

MC reweighting - B_c^+ kinematics reweighting

To correct the possible inaccuracy of the B_c^+ production in the MC simulation, the p_{T} and η distributions of the B_c^+ meson are measureed using the $B_c^+ \to J/\psi\pi^+$ events in both data and MC samples.

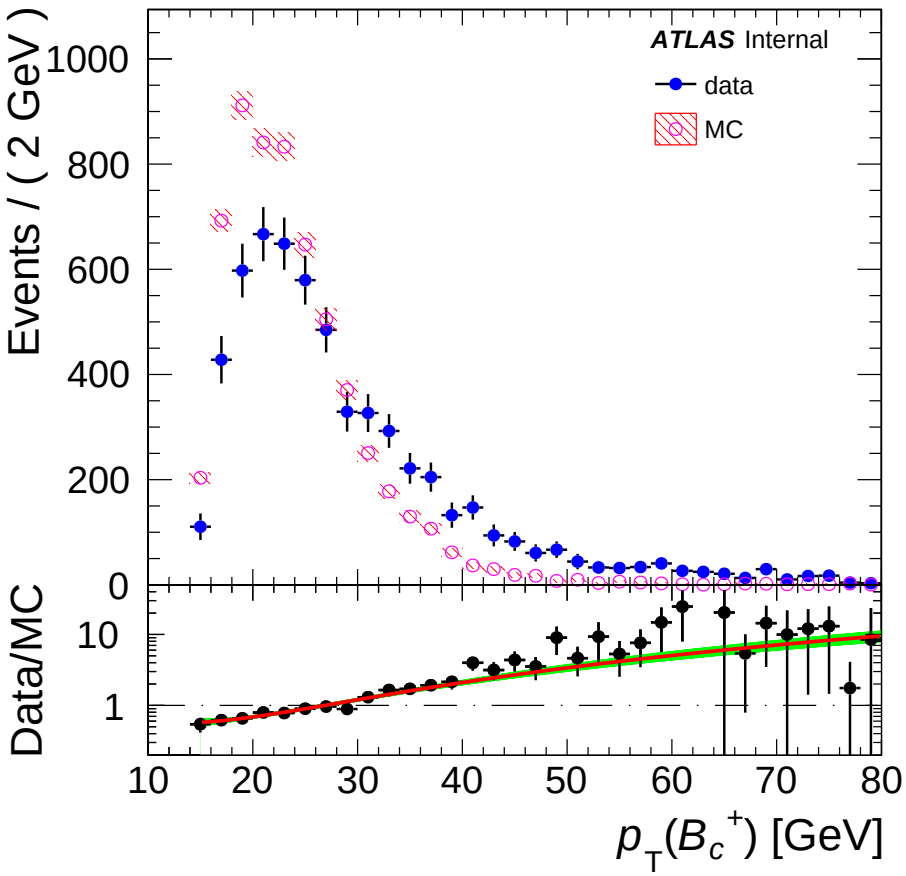

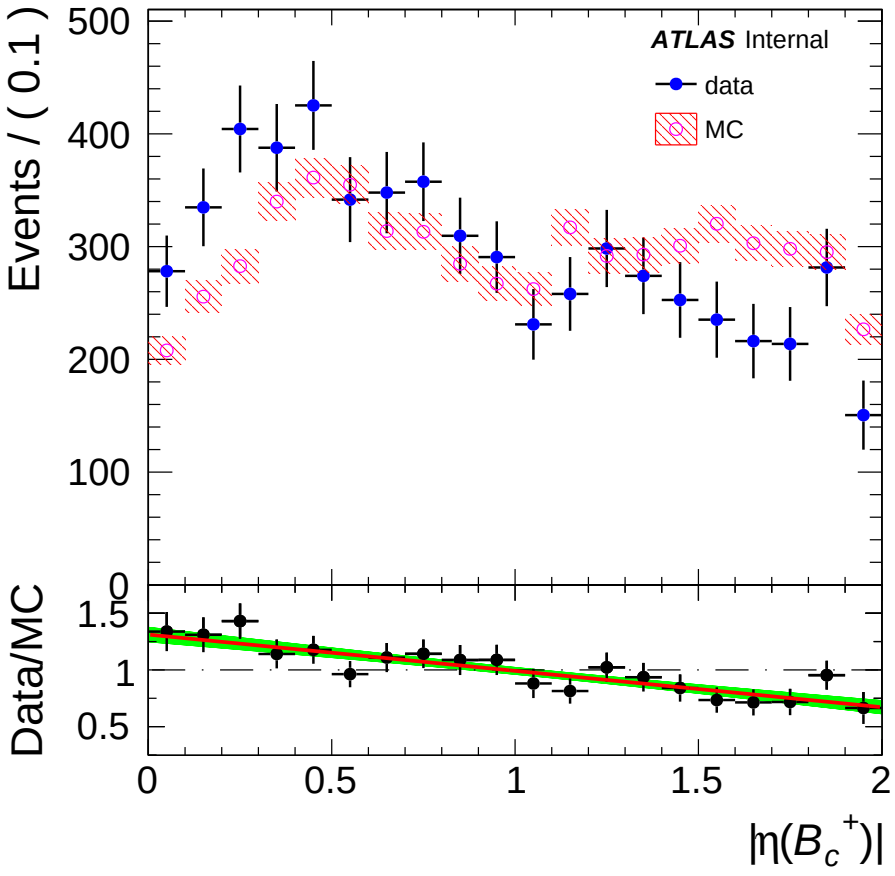

A weight calculated as a function of $p_{\mathrm{T}}(B_c^+)$ ($|\eta(B_c^+)|$) using the corresponding parameters is assigned to each simulated event in all decay modes.

MC reweighting - B_c^+ and D_s^+ lifetime reweighting

The proper lifetime of B_c^+ and D_s^+ mesons in the MC generation are defined by the settings in the EvtGen particle data table file. Those values are slightly different from the current world averages. To avoid the ect of this disagreement on the acceptances for each decay mode calculated from the MC, additional weights are introduced to correct the proper lifetime distributions. The weight for correction on proper lifetime is given by

$$w = \frac{\tau_{\mathrm{MC}}}{\tau_{\mathrm{PDG}}} \exp\left(-t\left(\frac{1}{\tau_{\mathrm{PDG}}} - \frac{1}{\tau_{\mathrm{MC}}}\right)\right),$$

where t is the actual proper lifetime of the truth B_c^+ (D_s^+) in the MC simulated events, τ_{MC} and τ_{PDG} are the average proper lifetime of B_c^+ (D_s^+) meson set in the generator and that from PDG, respectively.

Summary of acceptances

- **The acceptances for $B_c^+ \to J/\psi D_s^{*+}$ decay mode are considered separately for $\mathcal{A}_{\pm\pm}$ and $\mathcal{A}_{00}$ amplitudes. The overall acceptance of this mode is given by**

$$A_{B_c^+ \to J/\psi D_s^{*+}} = \frac{1}{f_{\pm\pm}/A_{\mathcal{A}_{\pm\pm}} + (1 - f_{\pm\pm}/A_{\mathcal{A}_{00}})},$$

where $f_{\pm\pm}$ is the value taken from the fit.

Mode	$A^{\rm gen}_{B_c^+ \to X}$ [%]	$A^{\rm rec}_{B_c^+ \to X}$ [%]	$A_{B_c^+ \to X}$ [%]
$B_c^+ \to J/\psi\pi^+$	34.64 ± 0.10	5.055 ± 0.070	1.751 ± 0.025
$B_c^+ \to J/\psi D_s^+$	27.97 ± 0.17	2.325 ± 0.094	0.650 ± 0.026
$B_c^+ \to J/\psi D_s^{*+}$, $\mathcal{A}_{00}$	27.19 ± 0.16	2.314 ± 0.093	0.629 ± 0.026
$B_c^+ \to J/\psi D_s^{*+}$, $\mathcal{A}_{\pm\pm}$	22.50 ± 0.11	2.687 ± 0.117	0.604 ± 0.027

Systematic uncertainty

- **MC modelling of B_c^+ production.**
  To correct for the possible difference in B_c^+ kinematics between data and MC simulation, the $p_{\mathrm{T}}(B_c^+)$ and $|\eta(B_c^+)|$ spectra are extracted using the abundant $B_c^+ \to J/\psi\pi^+$ channel. The differences in the $p_{\mathrm{T}}(B_c^+)$ and $|\eta(B_c^+)|$ spectra are then corrected for by reweighting the MC simulated events. The systematics arising from the acceptance correction is estimated by building the alternative acceptances with $\pm 1\sigma$ variations of correponding weights.
- **B_c^+ and D_s^+ lifetimes.**
  The limited knowledge of B_c^+ and D_s^+ lifetimes leads to an additional systematic uncertainty due to different decay time acceptances between the B_c^+ decay modes. The proper lifetime distributions of B_c^+ and D_s^+ mesons in the MC simulation are reweighed to vary the lifetimes within one standard deviation from the world average value.
- **Tracking efficiency uncertainty.**
  Another systematic uncertainty arises from the difference in the efficiencycyiency of track reconstruction and selection between data and MC. They are dominated by the uncertainty of the detector material description by the MC simulation. In order to evaluate the effect on the ratios of branching fractions, the difference in single-track reconstruction efficiency between data and MC provided by Combined Performance group are used to assign per-track weights to the signal and reference decay candidates.

Systematic uncertainty

- $B_c^+ \to J/\psi D_s^{(*)+}$ **signal fit.**
  To estimate the systematic uncertianites related to the fit model in $B_c^+ \to J/\psi D_s^{(*)+}$ decay mode, the fit has been performed with different models for the $J/\psi D_s^+$ signal: a double-Gaussian function, and a double-sided Crystal Ball function. The simulated templates of the $J/\psi D_s^{*+}$ signal shape has been varied by changing the smoothness parameter of the kernel estimate within a reasonable range. As alternative models for the background, the two-parameter exponential function, a second-order and a third-order polynomial functions are used.
- $B_c^+ \to J/\psi \pi^+$ **signal fit.**
  To estimate the systematic uncertianites related to the fit model in $B_c^+ \to J/\psi \pi^+$ mode, the fit has been performed with different models for the signal: a double-Gaussian function, and a double-sided Crystal Ball function. As alternative models for the background, a three-parameter exponential function, and a second-order polynomial function are used.
- **MC statistics.**
  The statistical uncertainties on the acceptance values due to limited MC statistics are also treated as a separate source of systematic uncertainty.
- $D_s^+ \to \phi(K^+K^-)\pi^+$ **branching fraction.**
  Its uncertainty is propagated to the final values of the relative branching fractions.

Systematic uncertainty

Source	Uncertainty [%]	
	$R_{D_s^+}$	$R_{D_s^{*+}}$
Simulated $p_{\mathrm{T}}(B_c^+)$ spectrum	0.5	0.1
Simulated $\lvert\eta(B_c^+)\rvert$ spectrum	0.2	0.2
B_c^+ lifetime	0.1	0.1
D_s^+ lifetime	0.2	0.1
Tracking efficency	0.8	0.7
$B_c^+ \to J/\psi D_s^{(*)+}$ signal fit		
– $B_c^+ \to J/\psi D_s^+$ signal shape	0.9	0.1
– $B_c^+ \to J/\psi D_s^{*+}$ signal shape	0.6	1.5
– Background shape	1.2	2.3
$B_c^+ \to J/\psi \pi^+$ signal fit		
– $B_c^+ \to J/\psi \pi^+$ signal shape	2.3	2.3
– Background shape	3.5	3.5
MC statistics	4.4	3.5
$\mathcal{B}(D_s^+ \to \phi(K^+K^-)\pi^+)$	3.5	3.5
Total	7.3	7.1

Branching ratios

The ratio of the branching fractions for $B_c^+ \to J/\psi D_s^{(*)+}$ and $J/\psi\pi^+$ is given by

$$\begin{aligned} R_{D_s^{(*)+}/\pi^+} &= \frac{\mathcal{B}(B_c^+ \to J/\psi D_s^{(*)+})}{\mathcal{B}(B_c^+ \to J/\psi\pi^+)} \\ &= \frac{N_{B_c^+ \to J/\psi D_s^{(*)+}}}{N_{B_c^+ \to J/\psi\pi^+}} \times \frac{A_{J/\psi\pi^+}}{A_{B_c^+ \to J/\psi D_s^{(*)+}}} \times \frac{1}{\mathcal{B}(D_s^+ \to \phi\pi^+)} \end{aligned}$$

The ratios of the branching fractions are measured to be

$$R_{D_s^+/\pi^+} = 3.63 \pm 0.58_{\mathbf{stat}} \pm 0.26_{\mathbf{syst}},$$

and

$$R_{D_s^{*+}/\pi^+} = 9.1 \pm 1.2_{\mathbf{stat}} \pm 0.6_{\mathbf{syst}}.$$

Summary

- **A study of $B_c^+ \to J/\psi D_s^{(*)+}$ decays has been performed by the ATLAS experiment at the LHC using pp collision data corresponding to an integrated luminosity of 140 fb^{-1} at 13 TeV centre-of-mass energy.**
- **Next to do:**
  - **Add mc16d and mc16e samples for $B_c^+ \to J/\psi D_s^{(*)+}$ channels**
  - **Optimize selection**
  - **Finish the analysis of $B_c^+ \to J/\psi D^{(*)+}$ decays**

Backup slides

Comparison

$R_{D_s^+/\pi^+}$	$R_{D_s^{*+}/\pi^+}$	$R_{D_s^{*+}/D_s^+}$	$\Gamma_{\pm\pm}/\Gamma$	Ref.
3.8 ± 1.2	10.4 ± 3.5	$2.8^{+1.2}_{-0.9}$	0.38 ± 0.24	ATLAS
2.90 ± 0.62	–	2.37 ± 0.57	0.52 ± 0.20	LHCb
2.6	4.5	1.7	–	QCD potential model
1.3	5.2	3.9	–	QCD sum rules
2.0	5.7	2.9	–	RCQM
2.2	–	–	–	BSW
2.06 ± 0.86	–	3.01 ± 1.23	–	LFQM
$3.45^{+0.49}_{-0.17}$	–	$2.54^{+0.07}_{-0.21}$	0.48 ± 0.04	pQCD
–	–	–	0.410	RIQM

Comparison

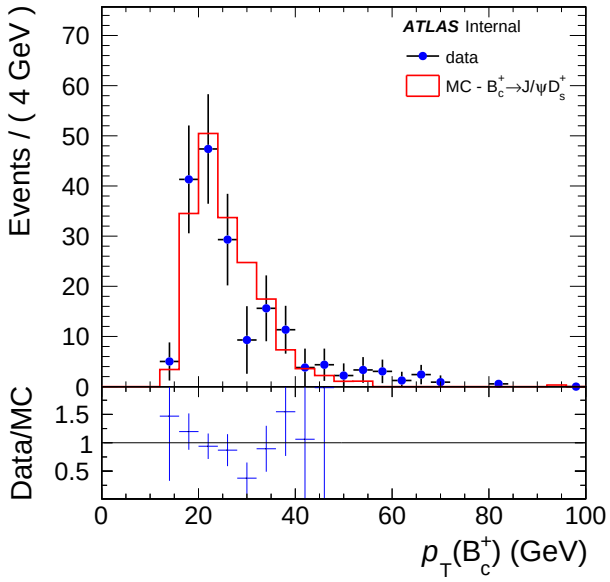
ATLAS Internal
data
MC - $B_c^+ \to J/\psi D_s^+$
Events / (4 GeV)
Data/MC
$p_T(B_c^+)$ (GeV)

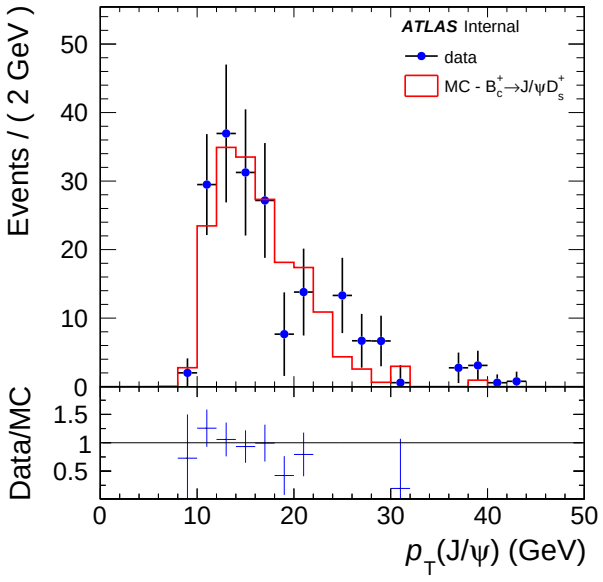
ATLAS Internal
data
MC - $B_c^+ \to J/\psi D_s^+$
Events / (2 GeV)
Data/MC
$p_T(J/\psi)$ (GeV)

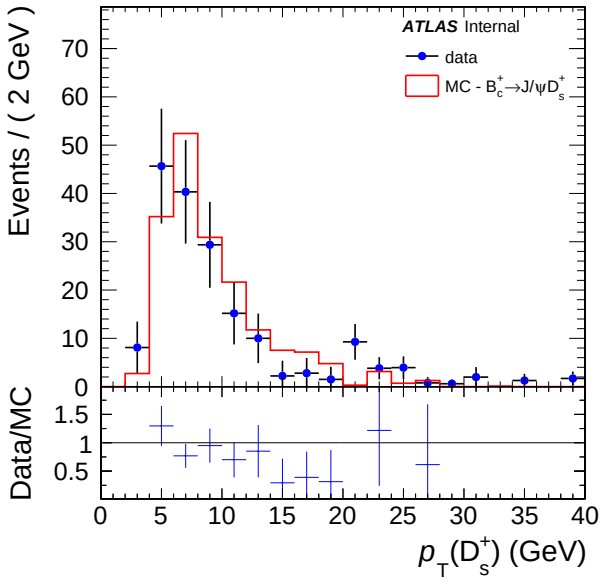
ATLAS Internal
data
MC - $B_c^+ \to J/\psi D_s^+$
Events / (2 GeV)
Data/MC
$p_T(D_s^+)$ (GeV)

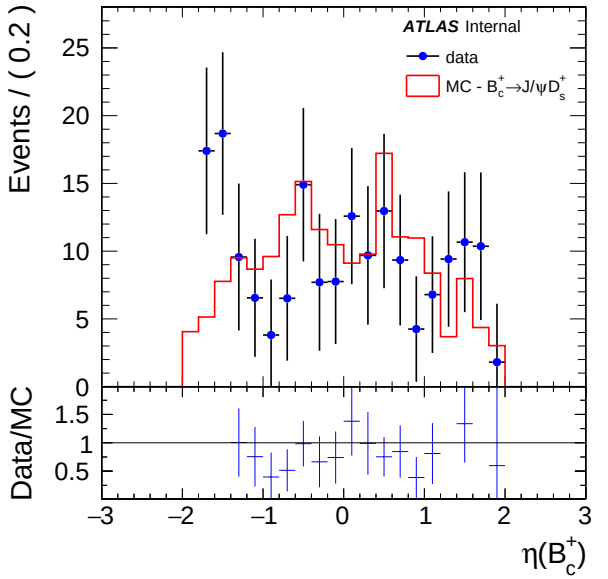
ATLAS Internal
data
MC - $B_c^+ \to J/\psi D_s^+$
Events / (0.2)
Data/MC
$\eta(B_c^+)$

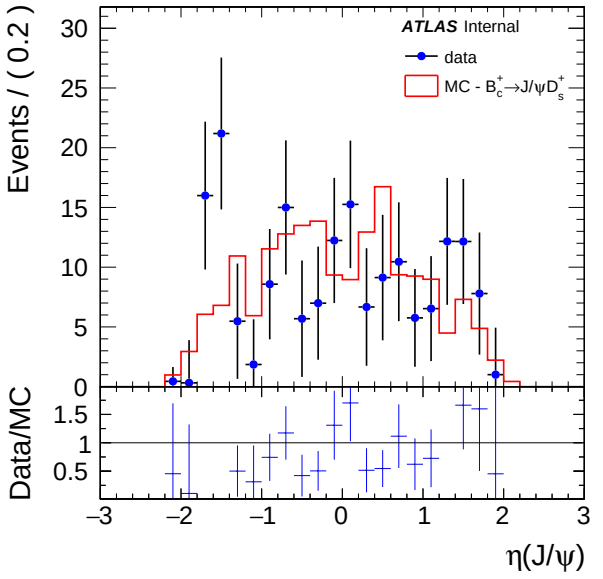
ATLAS Internal
data
MC - $B_c^+ \to J/\psi D_s^+$
Events / (0.2)
Data/MC
$\eta(J/\psi)$

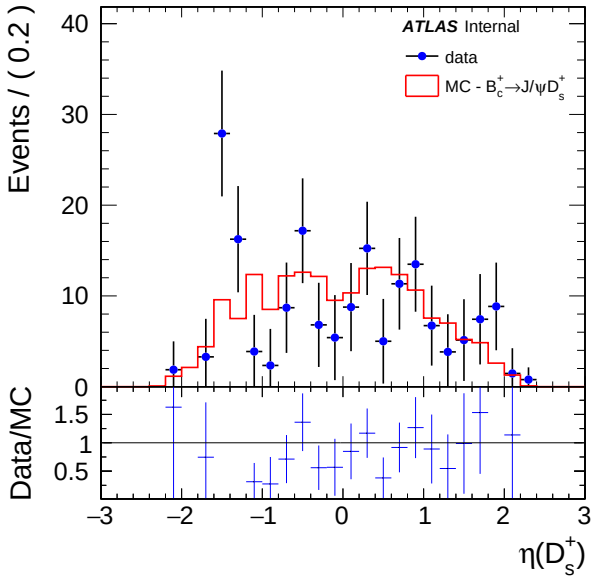
ATLAS Internal
data
MC - $B_c^+ \to J/\psi D_s^+$
Events / (0.2)
Data/MC
$\eta(D_s^+)$

Comparison

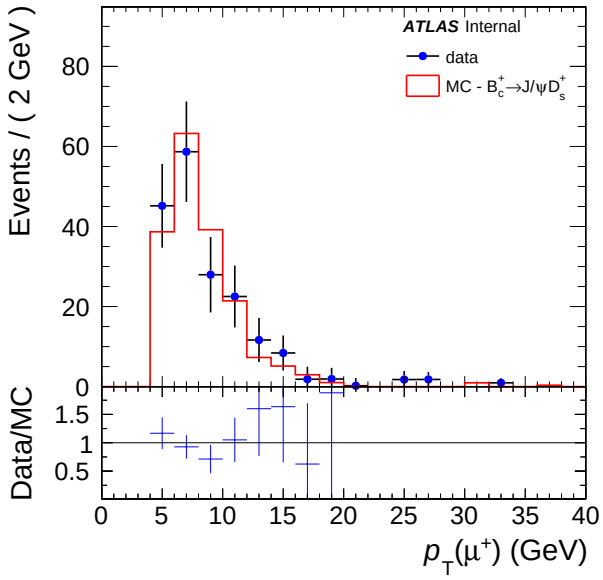
ATLAS Internal
data
MC - $B_c^+ \to J/\psi D_s^+$
Events / (2 GeV)
Data/MC
$p_T(\mu^+)$ (GeV)

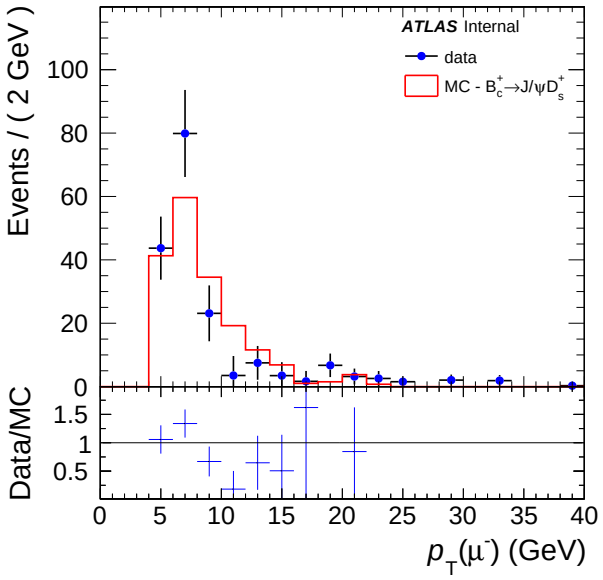
ATLAS Internal
data
MC - $B_c^+ \to J/\psi D_s^+$
Events / (2 GeV)
Data/MC
$p_T(\mu^-)$ (GeV)

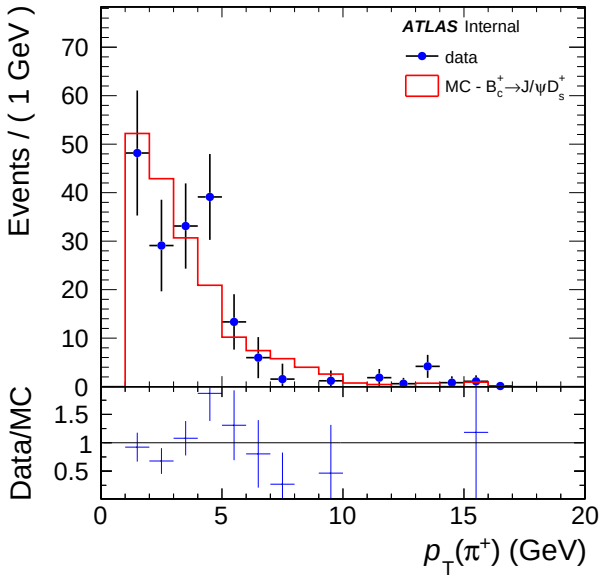
ATLAS Internal
data
MC - $B_c^+ \to J/\psi D_s^+$
Events / (1 GeV)
Data/MC
$p_T(\pi^+)$ (GeV)

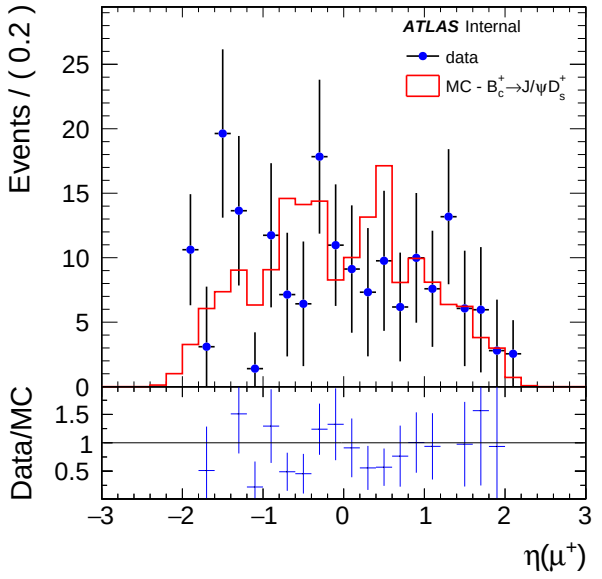
ATLAS Internal
data
MC - $B_c^+ \to J/\psi D_s^+$
Events / (0.2)
Data/MC
$\eta(\mu^+)$

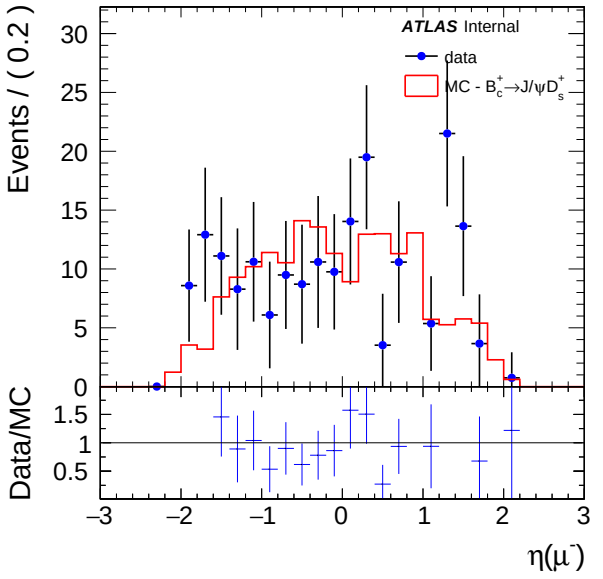
ATLAS Internal
data
MC - $B_c^+ \to J/\psi D_s^+$
Events / (0.2)
Data/MC
$\eta(\mu^-)$

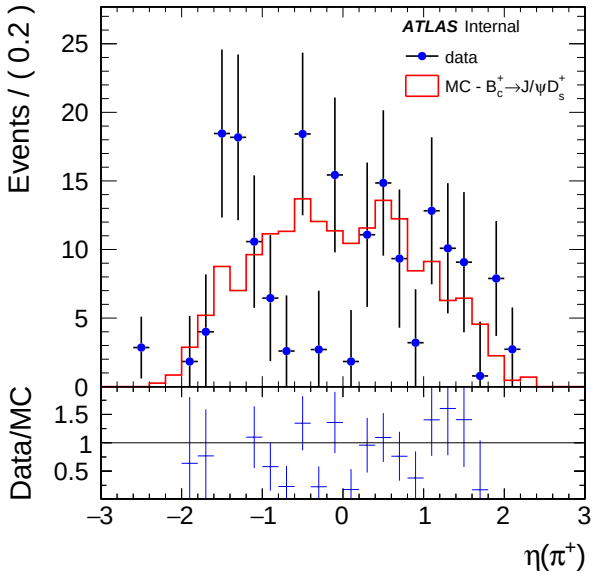
ATLAS Internal
data
MC - $B_c^+ \to J/\psi D_s^+$
Events / (0.2)
Data/MC
$\eta(\pi^+)$

Comparison

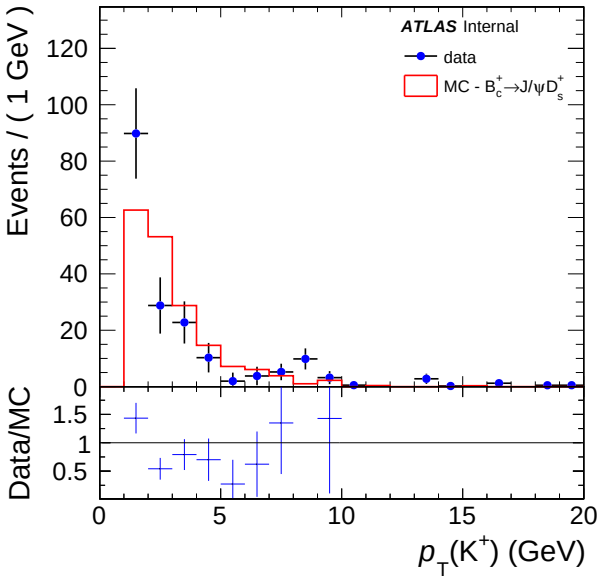
ATLAS Internal
data
MC - $B_c^+ \to J/\psi D_s^+$
Events / (1 GeV)
Data/MC
$p_T(K^+)$ (GeV)

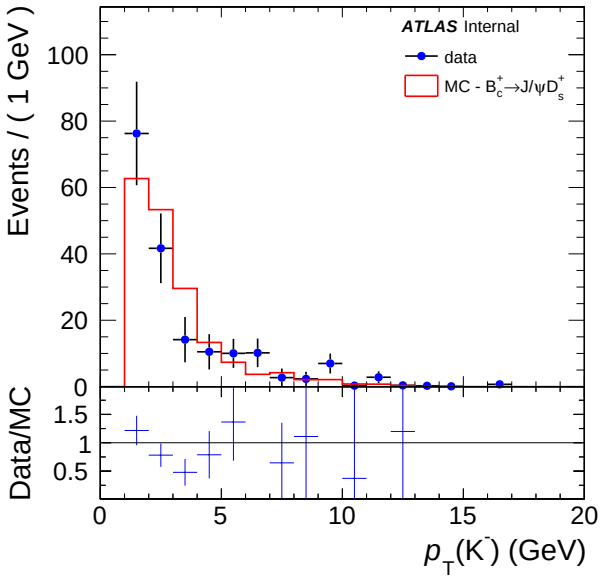
ATLAS Internal
data
MC - $B_c^+ \to J/\psi D_s^+$
Events / (1 GeV)
Data/MC
$p_T(K^-)$ (GeV)

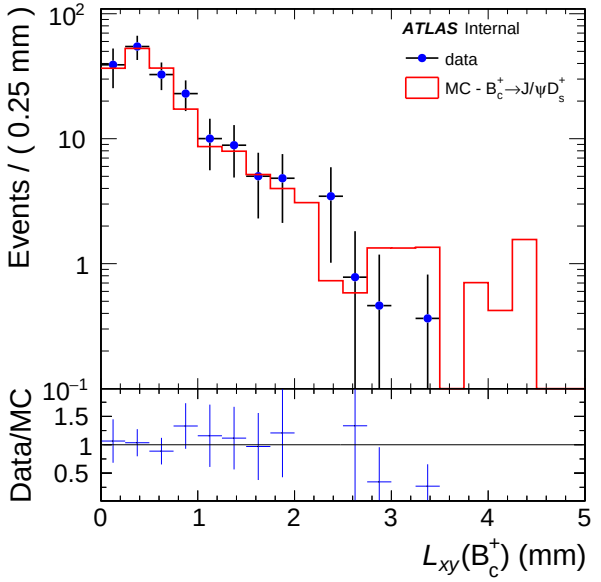
ATLAS Internal
data
MC - $B_c^+ \to J/\psi D_s^+$
Events / (0.25 mm)
Data/MC
$L_{xy}(B_c^+)$ (mm)

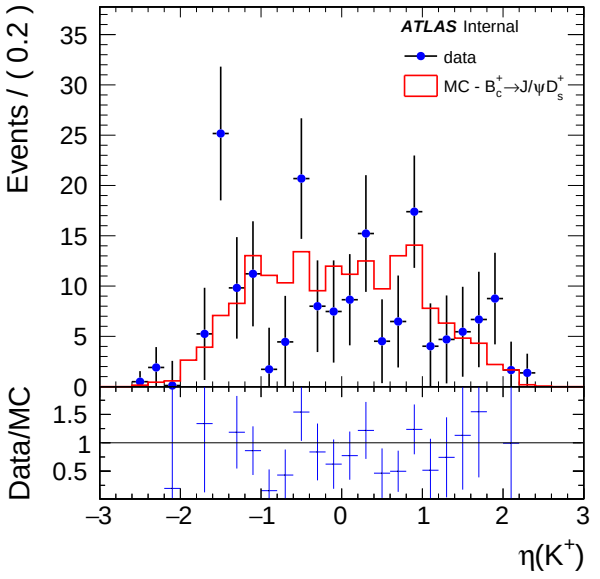
ATLAS Internal
data
MC - $B_c^+ \to J/\psi D_s^+$
Events / (0.2)
Data/MC
$\eta(K^+)$

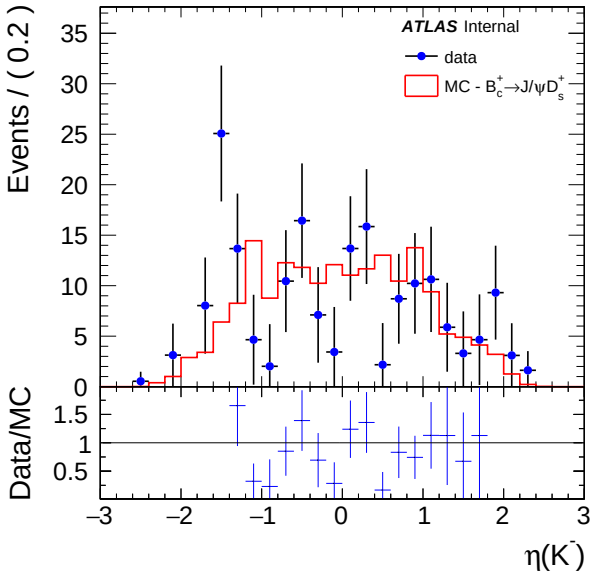
ATLAS Internal
data
MC - $B_c^+ \to J/\psi D_s^+$
Events / (0.2)
Data/MC
$\eta(K^-)$

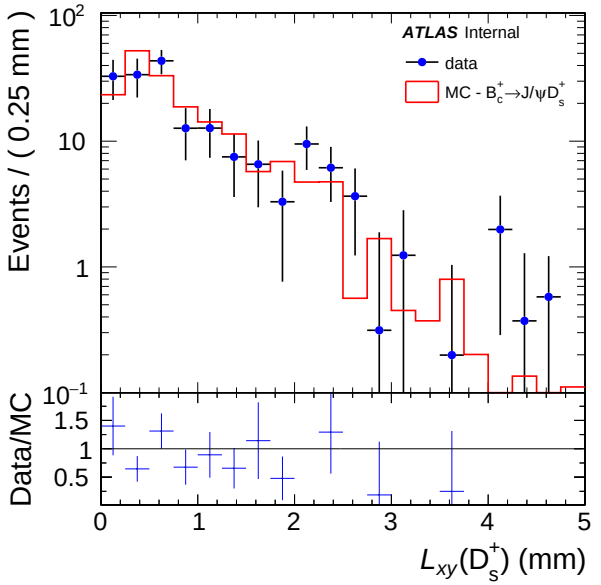
ATLAS Internal
data
MC - $B_c^+ \to J/\psi D_s^+$
Events / (0.25 mm)
Data/MC
$L_{xy}(D_s^+)$ (mm)

Comparison

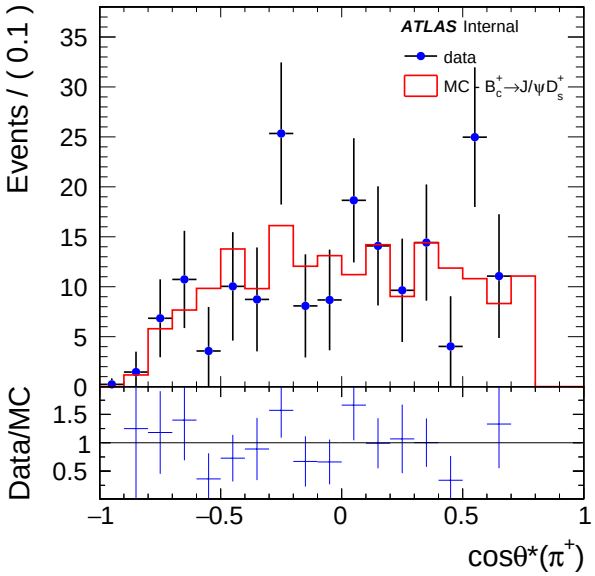
ATLAS Internal
data
MC - $B_c^+ \to J/\psi D_s^+$
Events / (0.1)
Data/MC
$\cos\theta^*(\pi^+)$

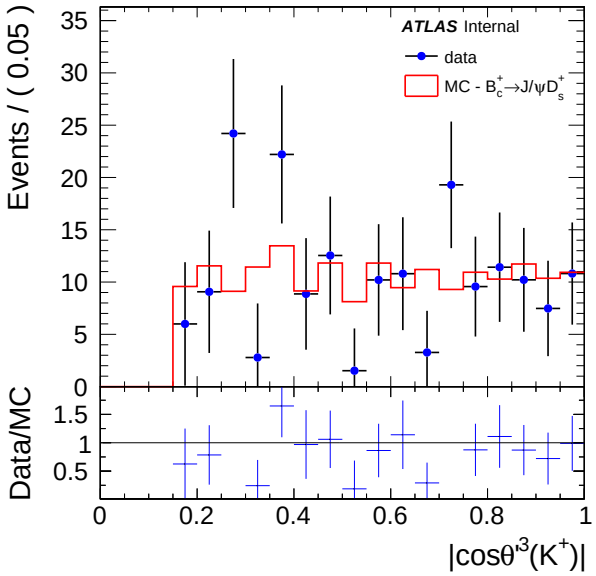
ATLAS Internal
data
MC - $B_c^+ \to J/\psi D_s^+$
Events / (0.05)
Data/MC
$|\cos\theta^3(K^+)|$

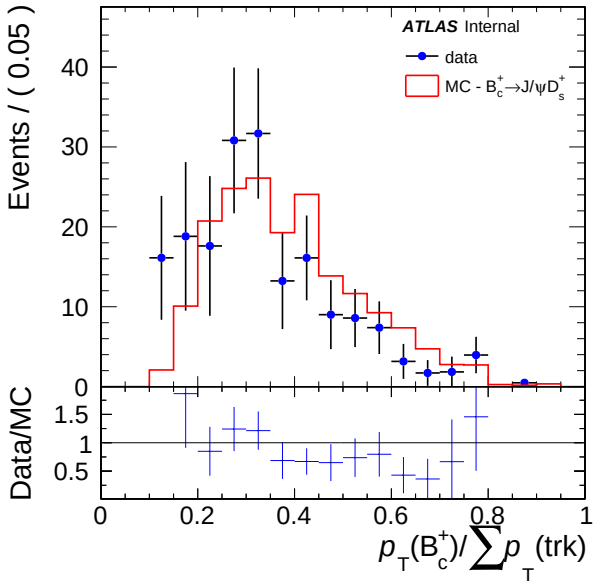
ATLAS Internal
data
MC - $B_c^+ \to J/\psi D_s^+$
Events / (0.05)
Data/MC
$p_T(B_c^+)/\sum p_T(\text{trk})$

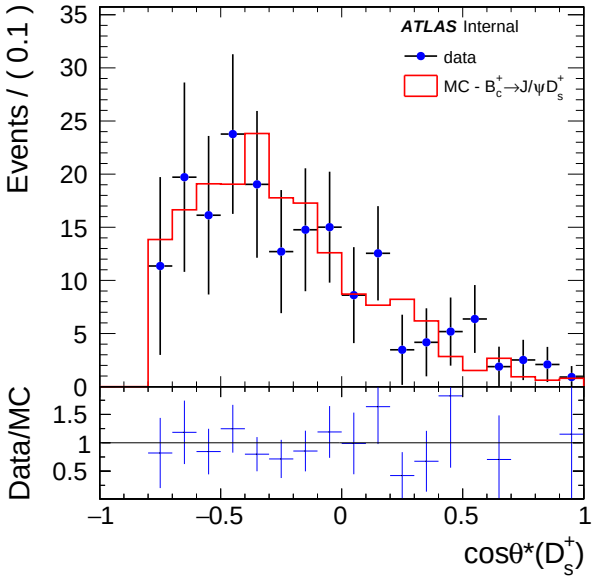
ATLAS Internal
data
MC - $B_c^+ \to J/\psi D_s^+$
Events / (0.1)
Data/MC
$\cos\theta^*(D_s^+)$

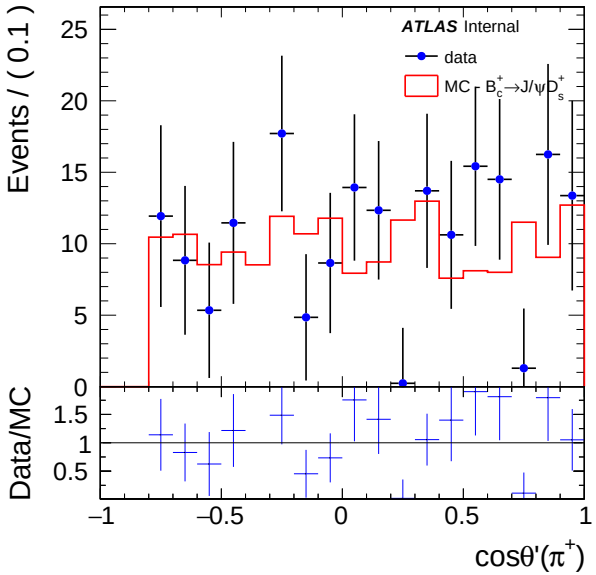
ATLAS Internal
data
MC - $B_c^+ \to J/\psi D_s^+$
Events / (0.1)
Data/MC
$\cos\theta'(\pi^+)$

Comparison

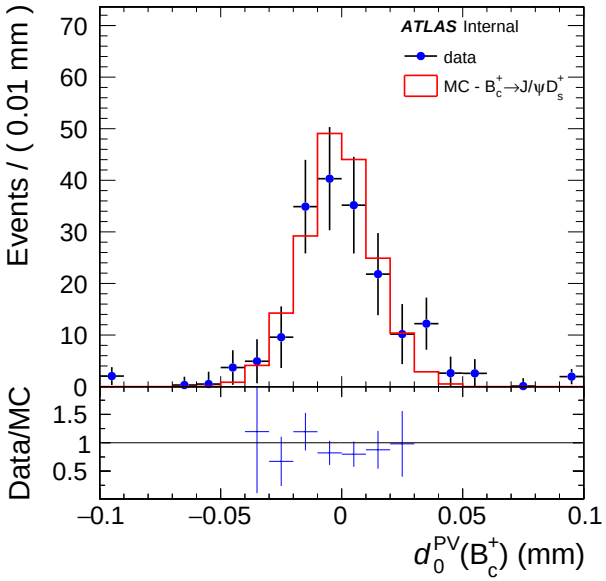
ATLAS Internal
data
MC - $B_c^+ \to J/\psi D_s^+$
Events / (0.01 mm)
Data/MC
$d_0^{PV}(B_c^+)$ (mm)

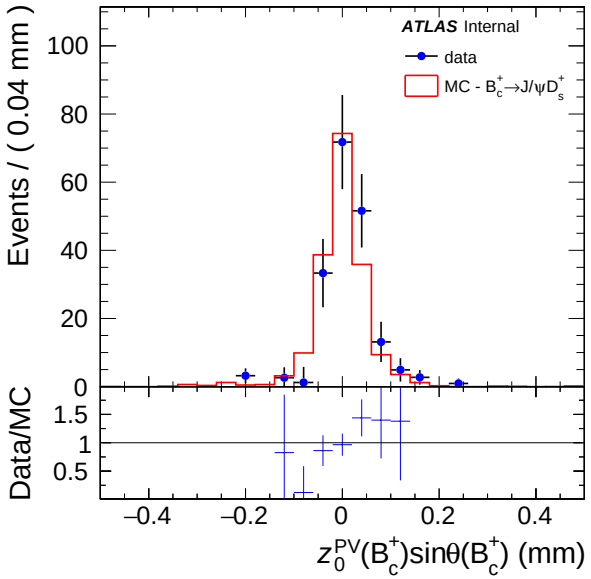
ATLAS Internal
data
MC - $B_c^+ \to J/\psi D_s^+$
Events / (0.04 mm)
Data/MC
$z_0^{PV}(B_c^+)\sin\theta(B_c^+)$ (mm)

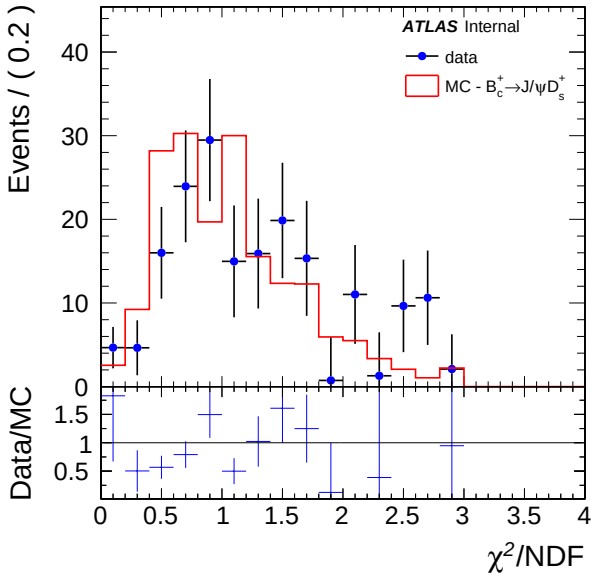
ATLAS Internal
data
MC - $B_c^+ \to J/\psi D_s^+$
Events / (0.2)
Data/MC
χ^2/NDF

Comparison

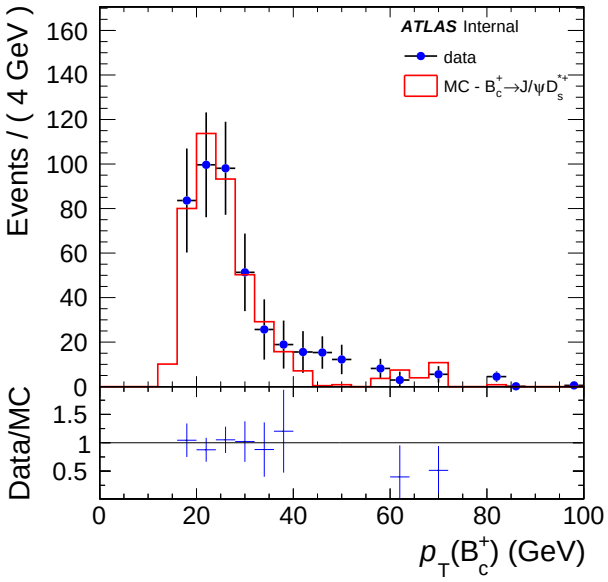
ATLAS Internal
data
MC - $B_c^+ \to J/\psi D_s^{*+}$
Events / (4 GeV)
Data/MC
$p_T(B_c^+)$ (GeV)

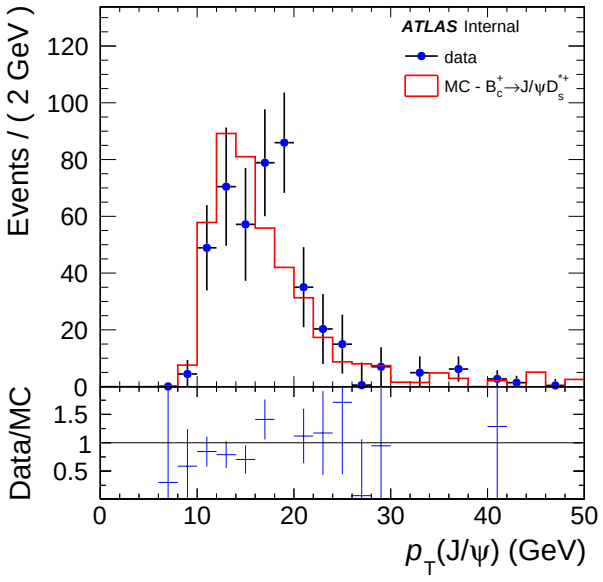
ATLAS Internal
data
MC - $B_c^+ \to J/\psi D_s^{*+}$
Events / (2 GeV)
Data/MC
$p_T(J/\psi)$ (GeV)

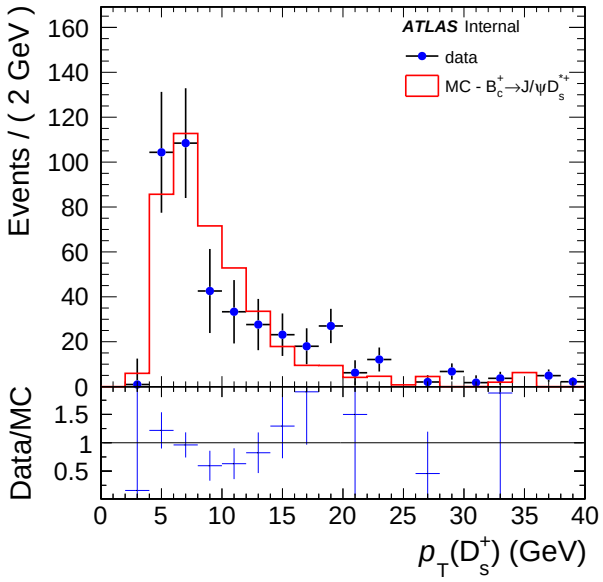
ATLAS Internal
data
MC - $B_c^+ \to J/\psi D_s^{*+}$
Events / (2 GeV)
Data/MC
$p_T(D_s^+)$ (GeV)

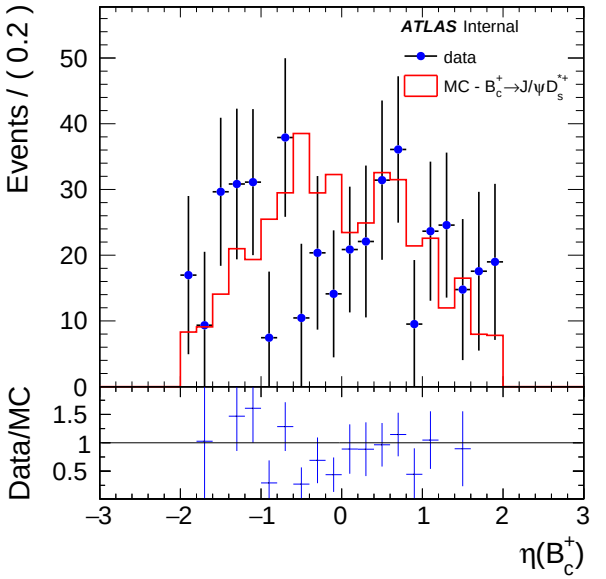
ATLAS Internal
data
MC - $B_c^+ \to J/\psi D_s^{*+}$
Events / (0.2)
Data/MC
$\eta(B_c^+)$

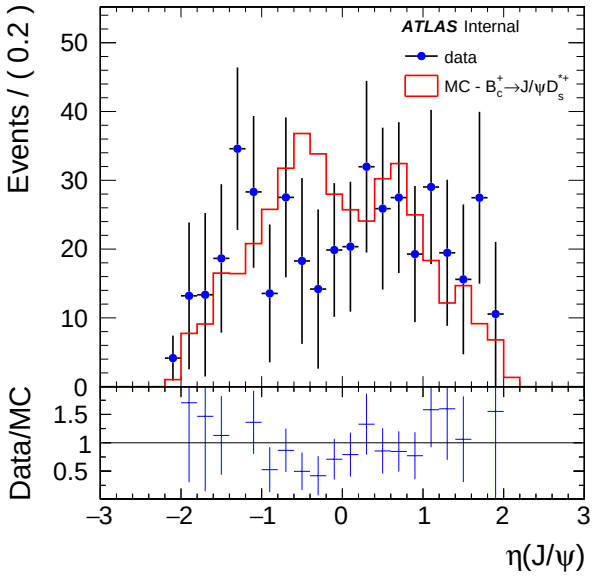
ATLAS Internal
data
MC - $B_c^+ \to J/\psi D_s^{*+}$
Events / (0.2)
Data/MC
$\eta(J/\psi)$

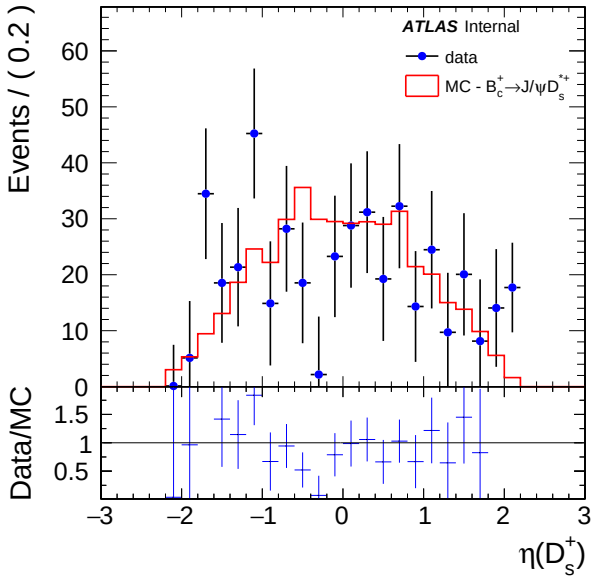
ATLAS Internal
data
MC - $B_c^+ \to J/\psi D_s^{*+}$
Events / (0.2)
Data/MC
$\eta(D_s^+)$

Comparison

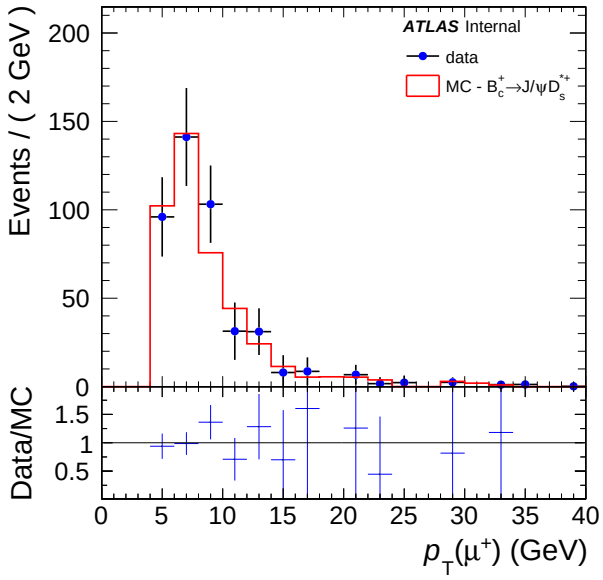
ATLAS Internal
data
MC - $B_c^+ \to J/\psi D_s^{*+}$
Events / (2 GeV)
Data/MC
$p_T(\mu^+)$ (GeV)

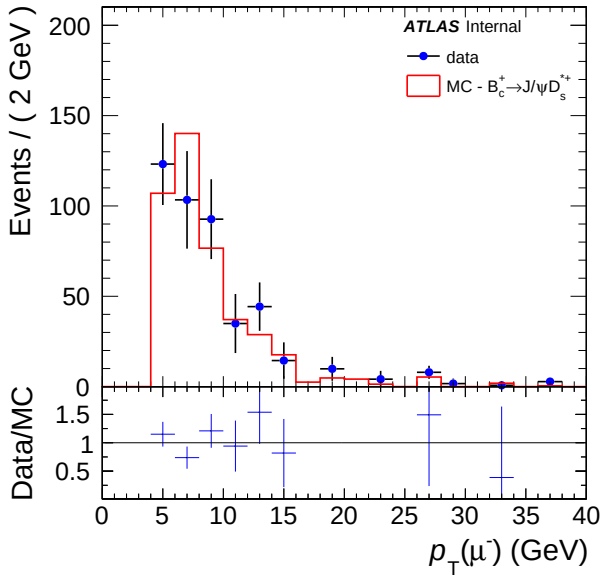
ATLAS Internal
data
MC - $B_c^+ \to J/\psi D_s^{*+}$
Events / (2 GeV)
Data/MC
$p_T(\mu^-)$ (GeV)

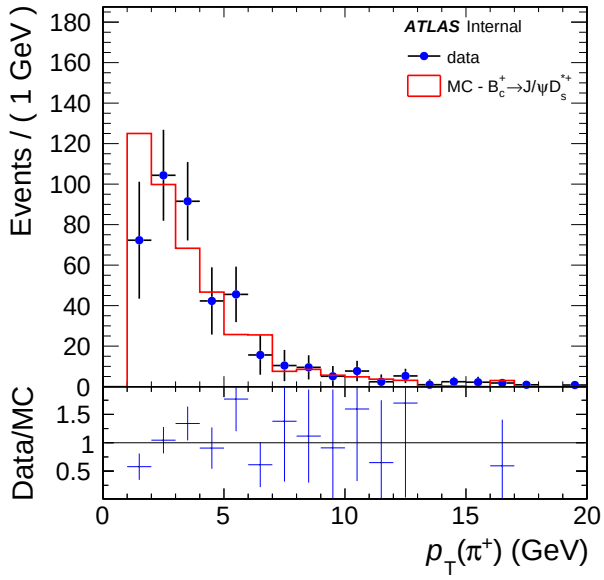
ATLAS Internal
data
MC - $B_c^+ \to J/\psi D_s^{*+}$
Events / (1 GeV)
Data/MC
$p_T(\pi^+)$ (GeV)

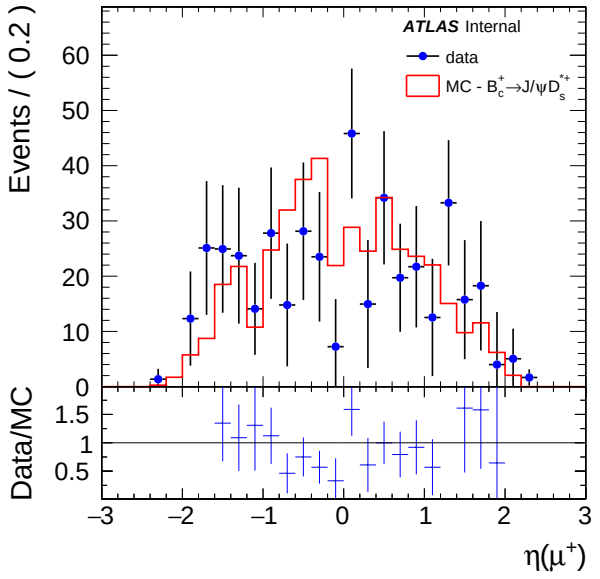
ATLAS Internal
data
MC - $B_c^+ \to J/\psi D_s^{*+}$
Events / (0.2)
Data/MC
$\eta(\mu^+)$

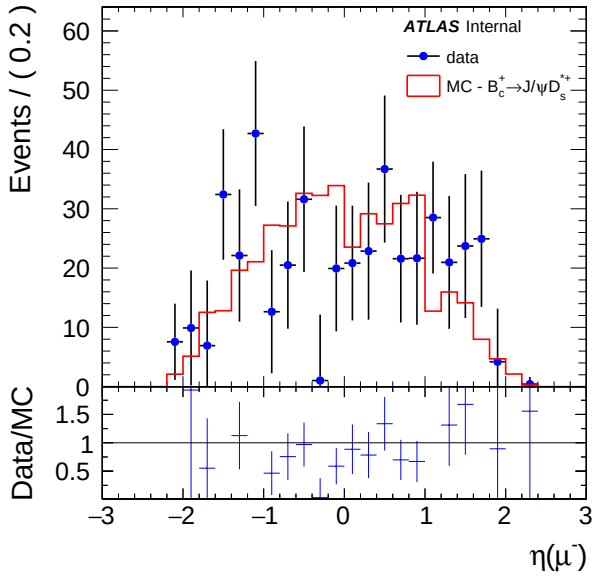
ATLAS Internal
data
MC - $B_c^+ \to J/\psi D_s^{*+}$
Events / (0.2)
Data/MC
$\eta(\mu^-)$

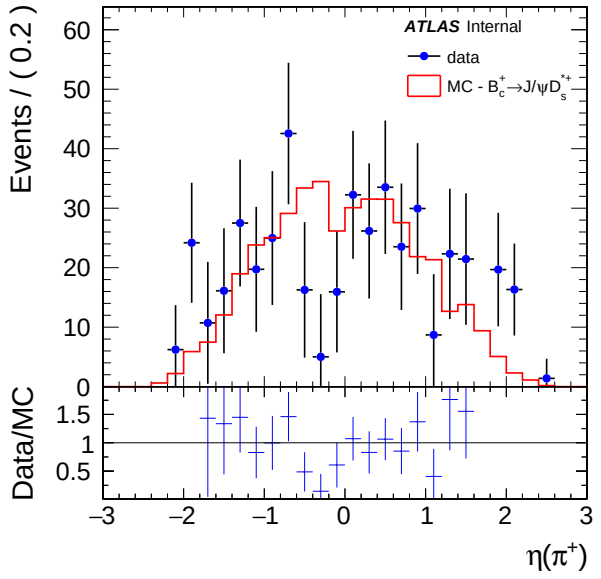
ATLAS Internal
data
MC - $B_c^+ \to J/\psi D_s^{*+}$
Events / (0.2)
Data/MC
$\eta(\pi^+)$

Comparison

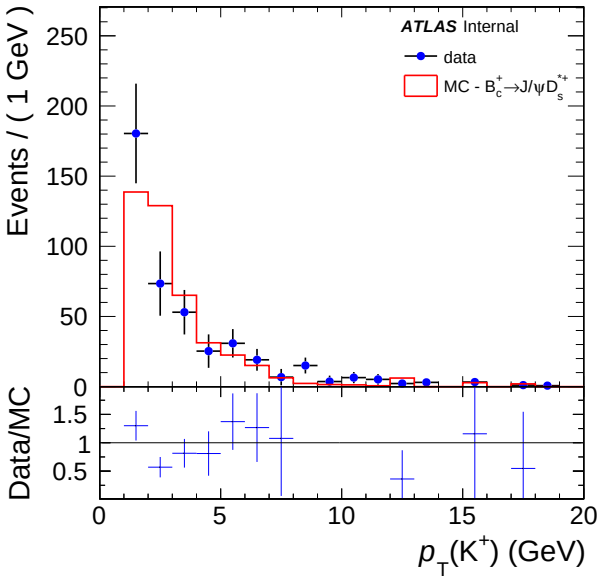
ATLAS Internal
data
MC - $B_c^+ \to J/\psi D_s^{*+}$
Events / (1 GeV)
Data/MC
$p_T(K^+)$ (GeV)

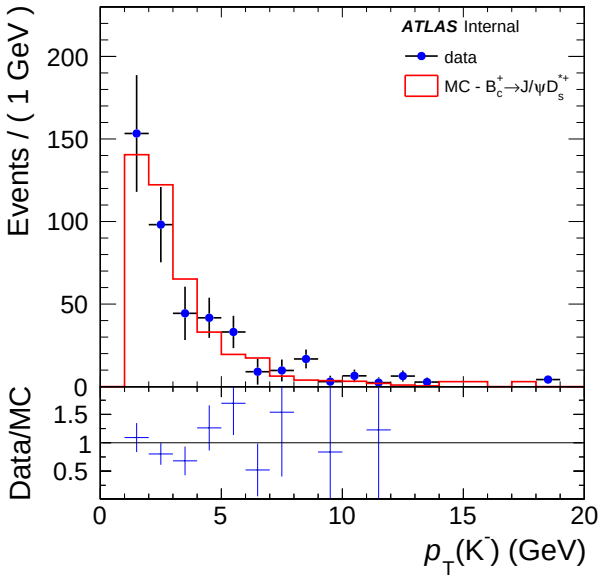
ATLAS Internal
data
MC - $B_c^+ \to J/\psi D_s^{*+}$
Events / (1 GeV)
Data/MC
$p_T(K^-)$ (GeV)

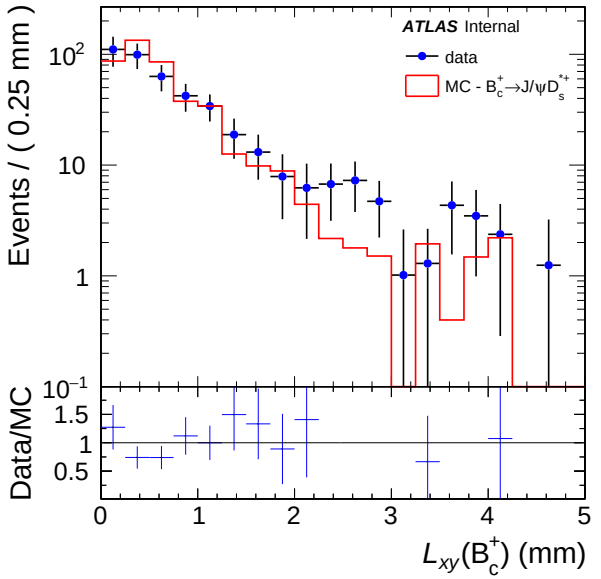
ATLAS Internal
data
MC - $B_c^+ \to J/\psi D_s^{*+}$
Events / (0.25 mm)
Data/MC
$L_{xy}(B_c^+)$ (mm)

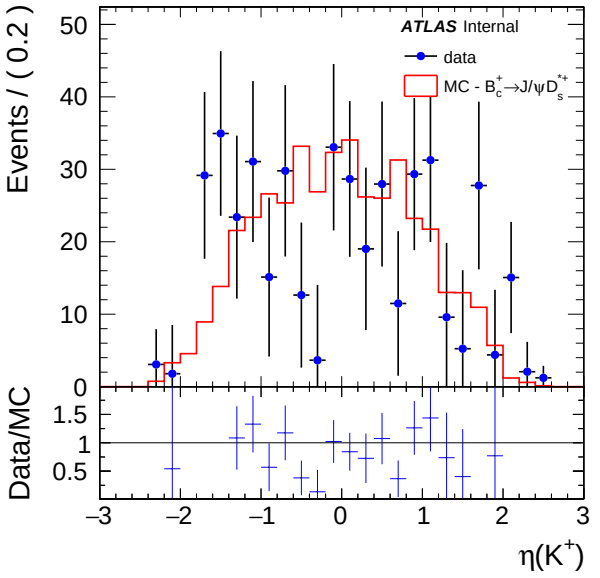
ATLAS Internal
data
MC - $B_c^+ \to J/\psi D_s^{*+}$
Events / (0.2)
Data/MC
$\eta(K^+)$

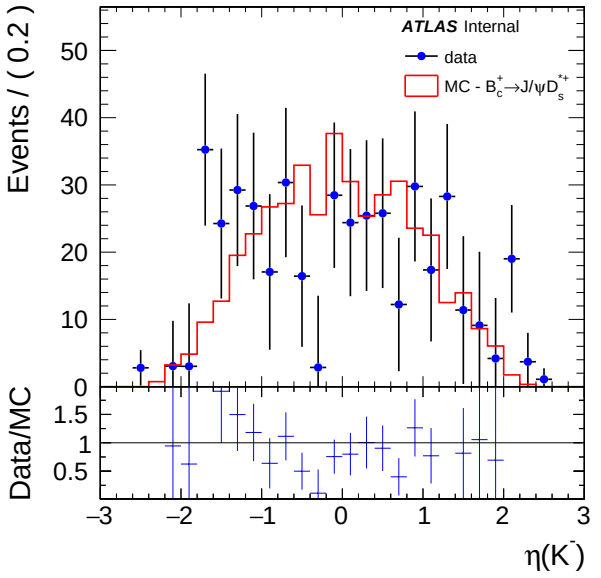
ATLAS Internal
data
MC - $B_c^+ \to J/\psi D_s^{*+}$
Events / (0.2)
Data/MC
$\eta(K^-)$

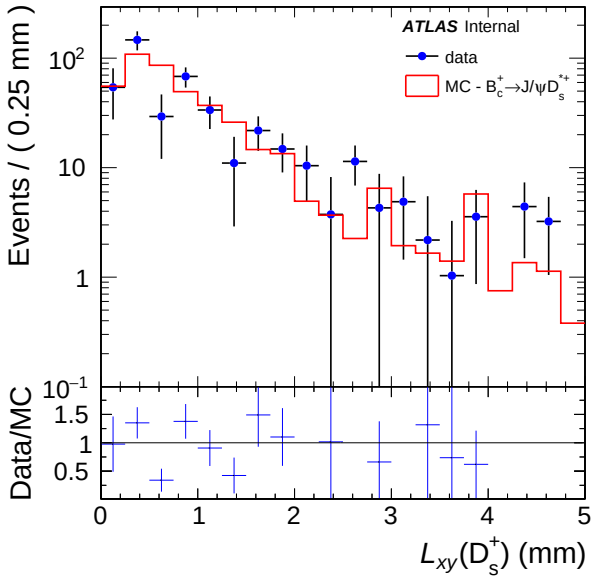
ATLAS Internal
data
MC - $B_c^+ \to J/\psi D_s^{*+}$
Events / (0.25 mm)
Data/MC
$L_{xy}(D_s^+)$ (mm)

Comparison

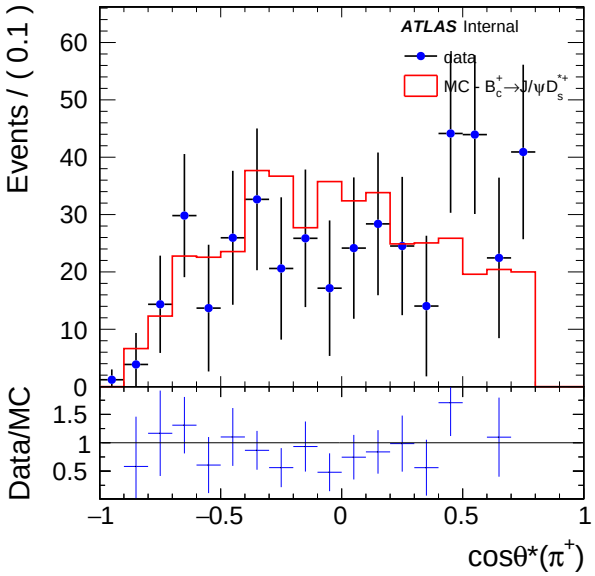
ATLAS Internal
data
MC - $B_c^+ \to J/\psi D_s^{*+}$
Events / (0.1)
Data/MC
$\cos\theta^*(\pi^+)$

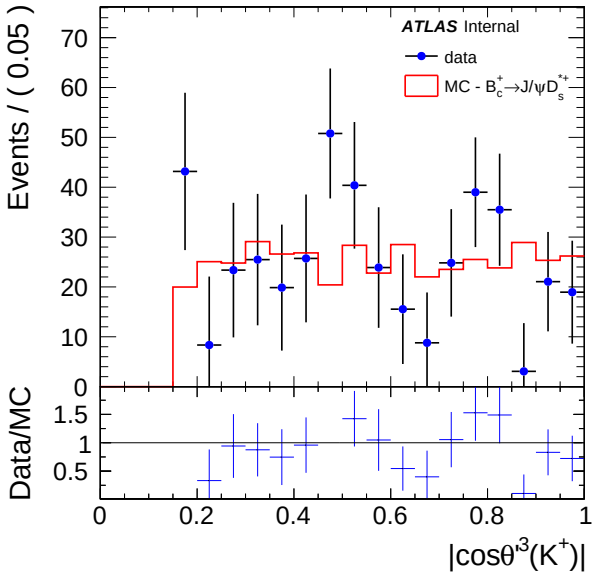
ATLAS Internal
data
MC - $B_c^+ \to J/\psi D_s^{*+}$
Events / (0.05)
Data/MC
$|\cos\theta^3(K^+)|$

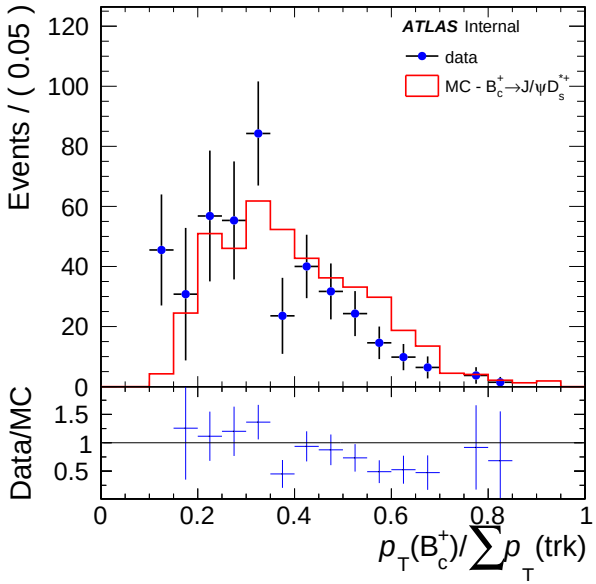
ATLAS Internal
data
MC - $B_c^+ \to J/\psi D_s^{*+}$
Events / (0.05)
Data/MC
$p_T(B_c^+)/\sum p_T(\mathrm{trk})$

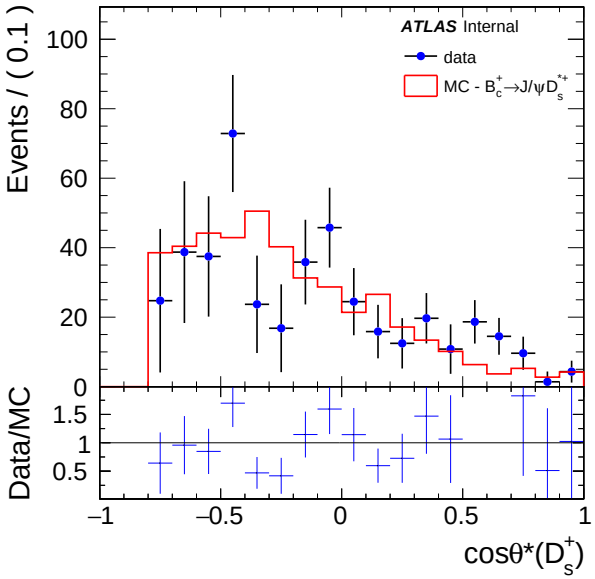
ATLAS Internal
data
MC - $B_c^+ \to J/\psi D_s^{*+}$
Events / (0.1)
Data/MC
$\cos\theta^*(D_s^+)$

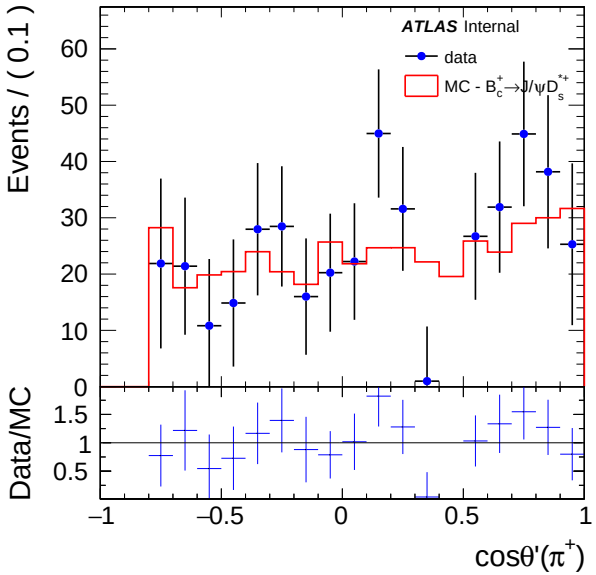
ATLAS Internal
data
MC - $B_c^+ \to J/\psi D_s^{*+}$
Events / (0.1)
Data/MC
$\cos\theta'(\pi^+)$

Comparison

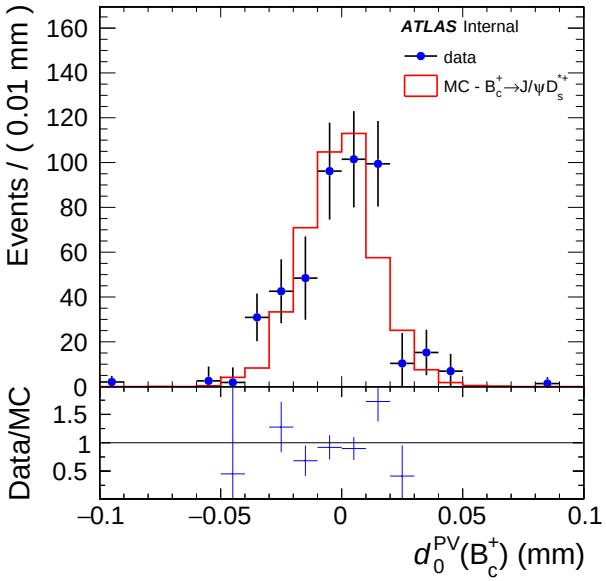
ATLAS Internal
data
MC - $B_c^+ \to J/\psi D_s^{*+}$
Events / (0.01 mm)
Data/MC
$d_0^{PV}(B_c^+)$ (mm)

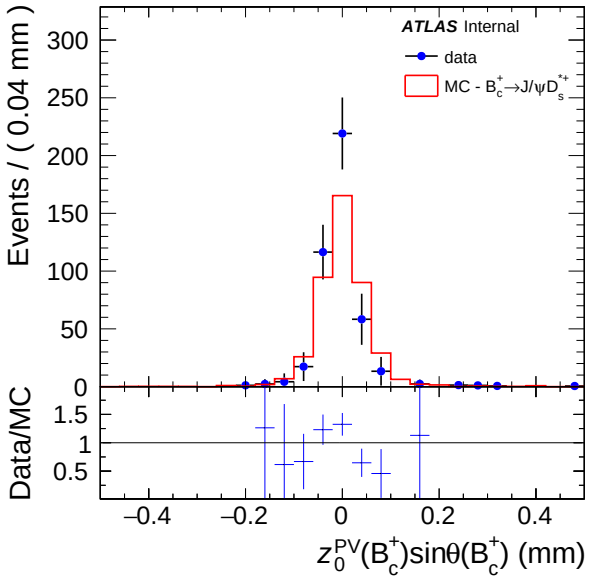
ATLAS Internal
data
MC - $B_c^+ \to J/\psi D_s^{*+}$
Events / (0.04 mm)
Data/MC
$z_0^{PV}(B_c^+)\sin\theta(B_c^+)$ (mm)

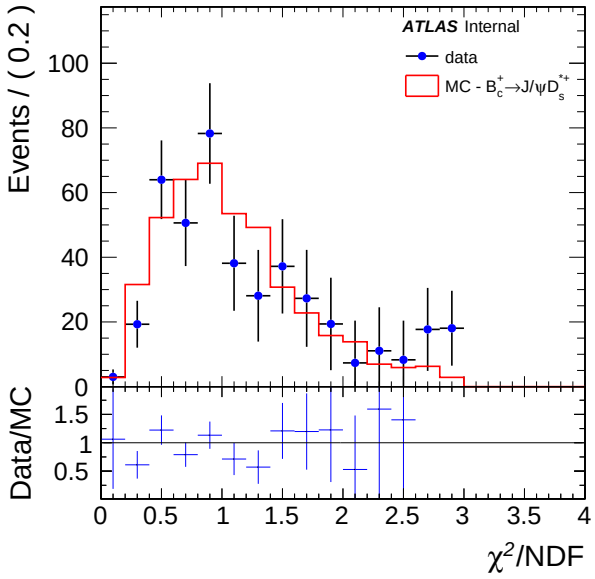
ATLAS Internal
data
MC - $B_c^+ \to J/\psi D_s^{*+}$
Events / (0.2)
Data/MC
χ^2/NDF

Comparison

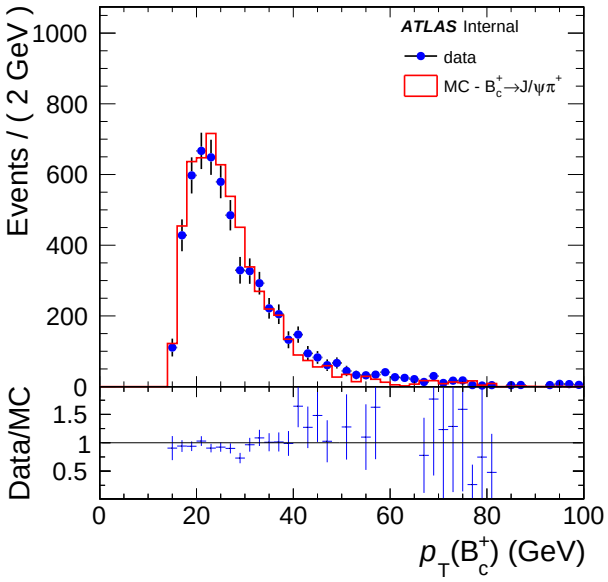
ATLAS Internal
data
MC - $B_c^+ \to J/\psi\pi^+$
Events / (2 GeV)
Data/MC
$p_T(B_c^+)$ (GeV)

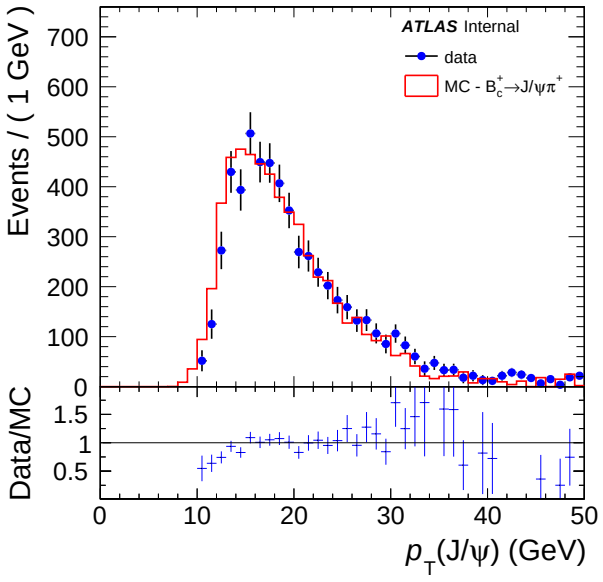
ATLAS Internal
data
MC - $B_c^+ \to J/\psi\pi^+$
Events / (1 GeV)
Data/MC
$p_T(J/\psi)$ (GeV)

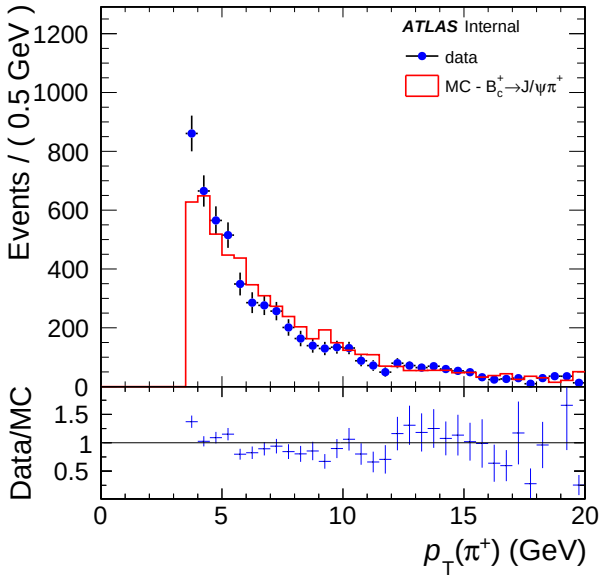
ATLAS Internal
data
MC - $B_c^+ \to J/\psi\pi^+$
Events / (0.5 GeV)
Data/MC
$p_T(\pi^+)$ (GeV)

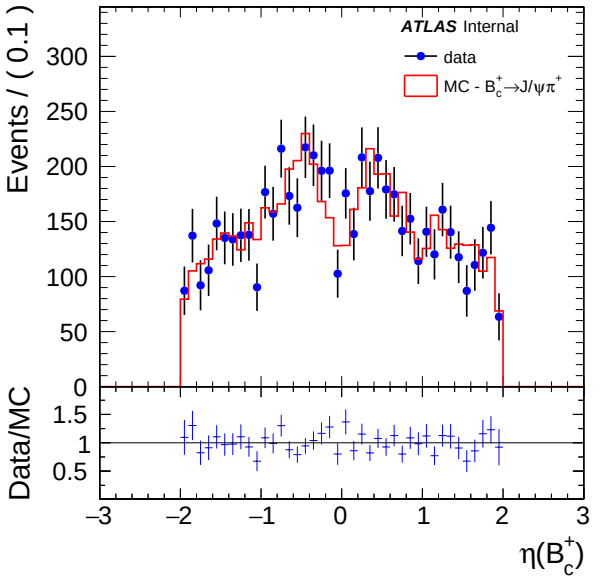
ATLAS Internal
data
MC - $B_c^+ \to J/\psi\pi^+$
Events / (0.1)
Data/MC
$\eta(B_c^+)$

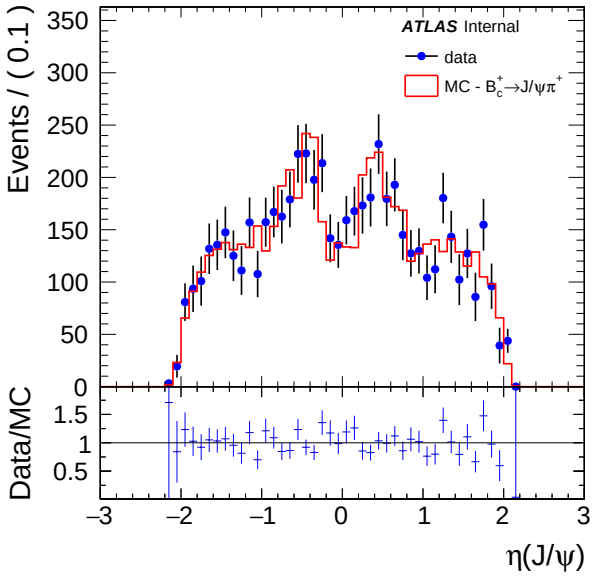
ATLAS Internal
data
MC - $B_c^+ \to J/\psi\pi^+$
Events / (0.1)
Data/MC
$\eta(J/\psi)$

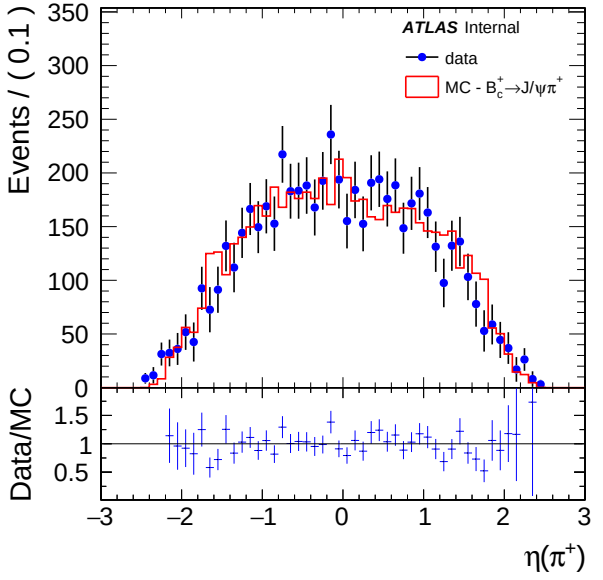
ATLAS Internal
data
MC - $B_c^+ \to J/\psi\pi^+$
Events / (0.1)
Data/MC
$\eta(\pi^+)$

Comparison

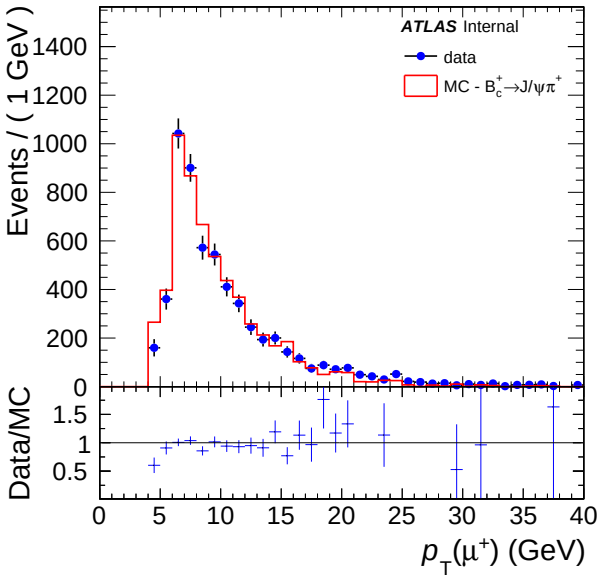
ATLAS Internal
data
MC - $B_c^+ \to J/\psi\pi^+$
Events / (1 GeV)
Data/MC
$p_T(\mu^+)$ (GeV)

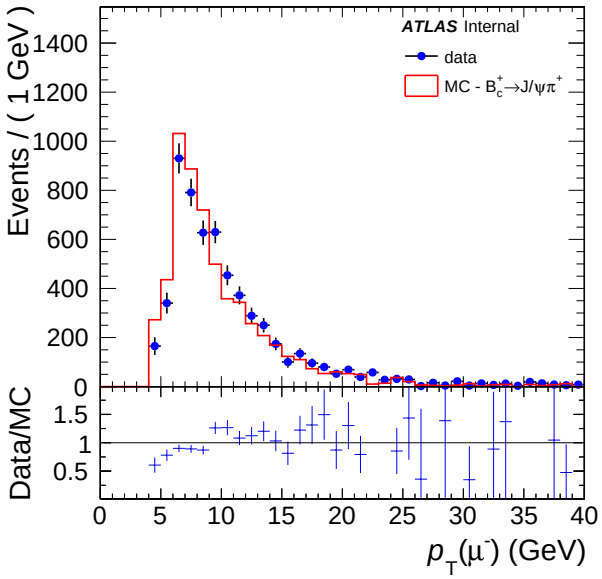
ATLAS Internal
data
MC - $B_c^+ \to J/\psi\pi^+$
Events / (1 GeV)
Data/MC
$p_T(\mu^-)$ (GeV)

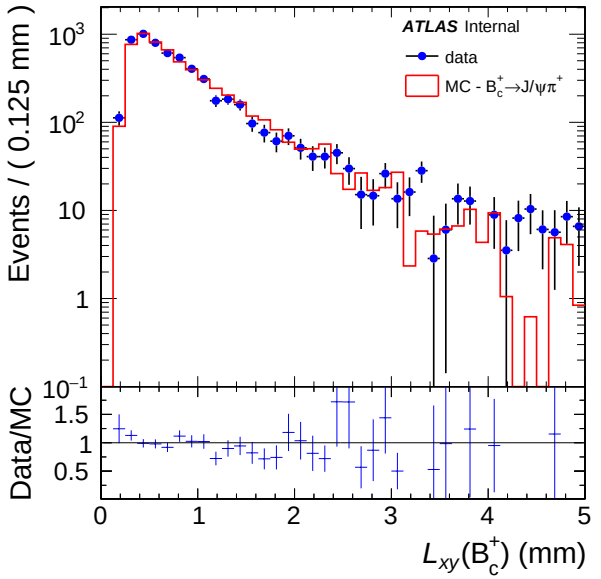
ATLAS Internal
data
MC - $B_c^+ \to J/\psi\pi^+$
Events / (0.125 mm)
Data/MC
$L_{xy}(B_c^+)$ (mm)

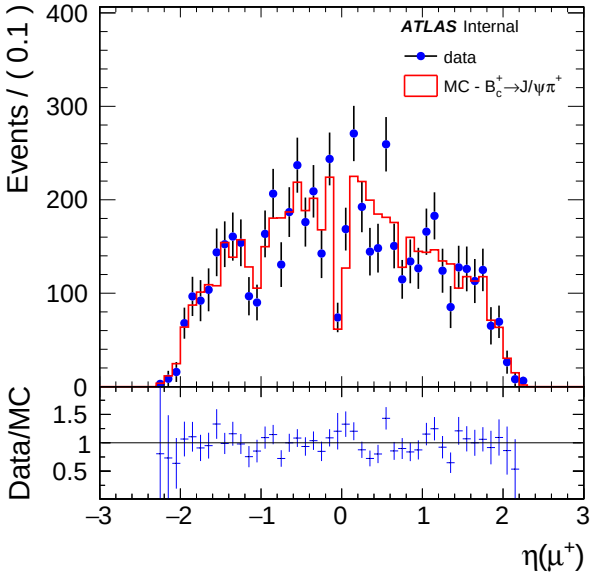
ATLAS Internal
data
MC - $B_c^+ \to J/\psi\pi^+$
Events / (0.1)
Data/MC
$\eta(\mu^+)$

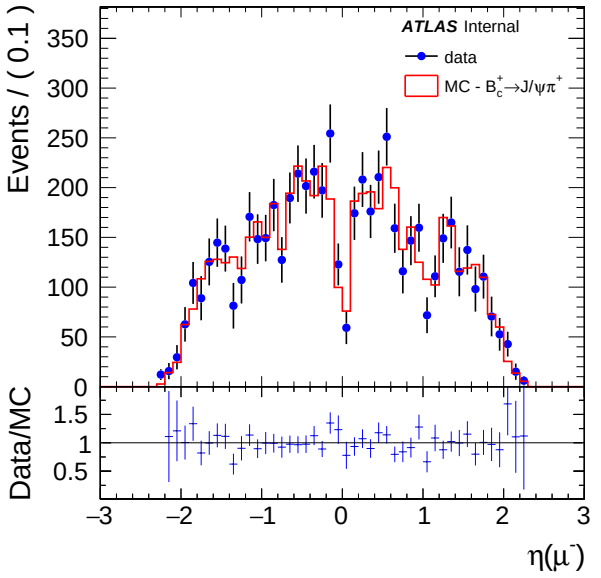
ATLAS Internal
data
MC - $B_c^+ \to J/\psi\pi^+$
Events / (0.1)
Data/MC
$\eta(\mu^-)$

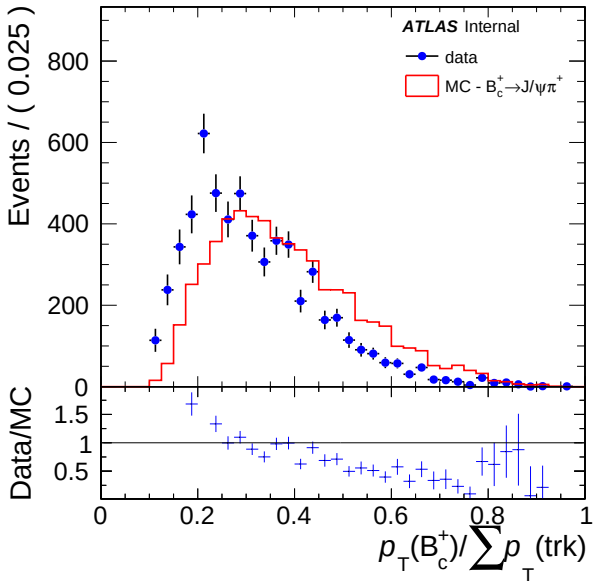
ATLAS Internal
data
MC - $B_c^+ \to J/\psi\pi^+$
Events / (0.025)
Data/MC
$p_T(B_c^+)/\sum p_T$ (trk)

Comparison

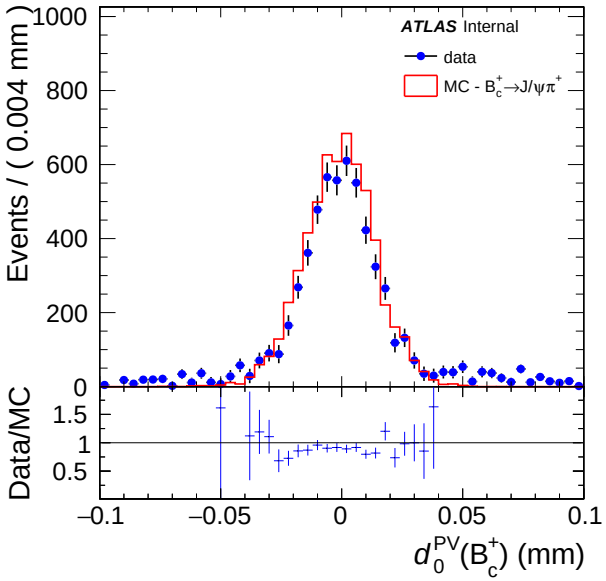
ATLAS Internal
data
MC - $B_c^+ \to J/\psi\pi^+$
Events / (0.004 mm)
Data/MC
$d_0^{PV}(B_c^+)$ (mm)

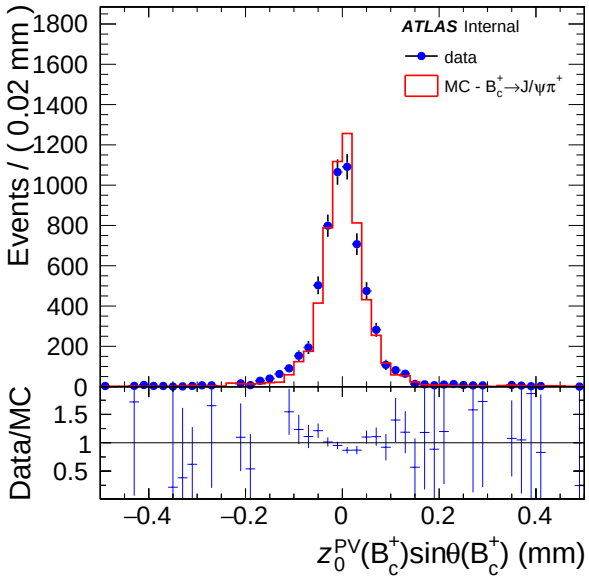
ATLAS Internal
data
MC - $B_c^+ \to J/\psi\pi^+$
Events / (0.02 mm)
Data/MC
$z_0^{PV}(B_c^+)\sin\theta(B_c^+)$ (mm)

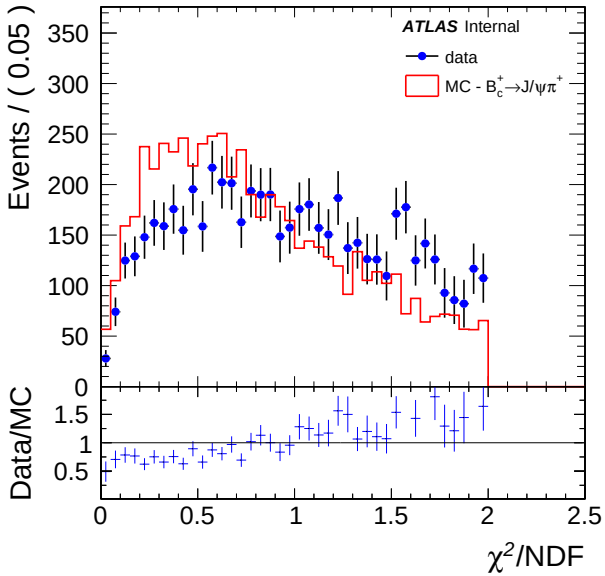
ATLAS Internal
data
MC - $B_c^+ \to J/\psi\pi^+$
Events / (0.05)
Data/MC
χ^2/NDF

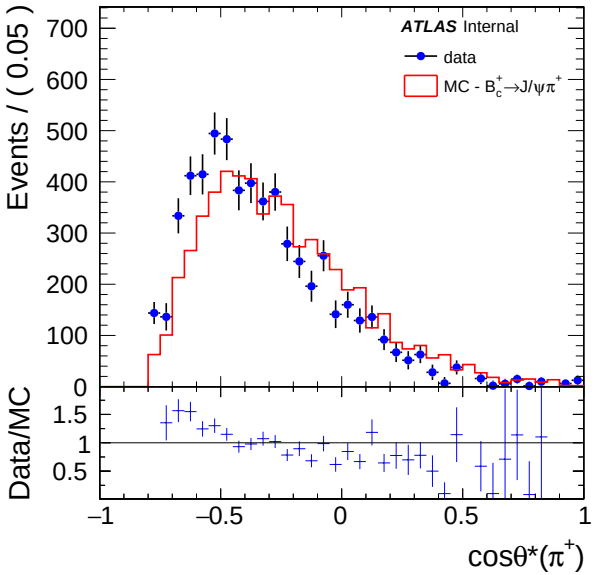
ATLAS Internal
data
MC - $B_c^+ \to J/\psi\pi^+$
Events / (0.05)
Data/MC
$\cos\theta^*(\pi^+)$

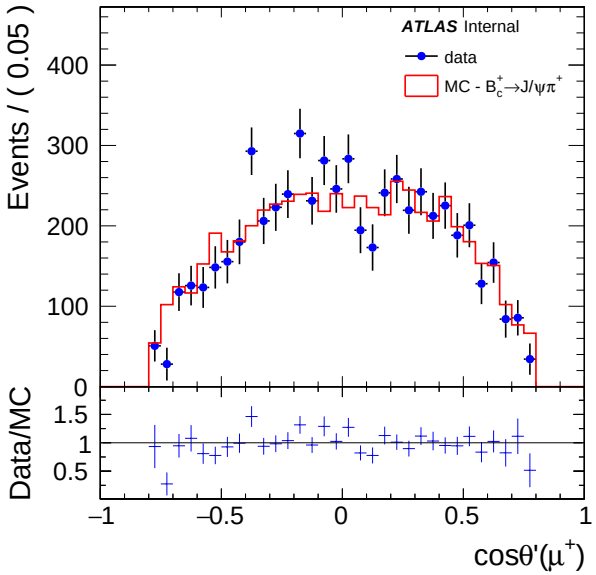
ATLAS Internal
data
MC - $B_c^+ \to J/\psi\pi^+$
Events / (0.05)
Data/MC
$\cos\theta'(\mu^+)$